Reverse Link Analysis and Modeling of CDMA based Distributed Antenna Systems

by

Blaze Vincent

B.Tech, University of Calicut, India, 2006

A thesis submitted to the

Faculty of the Graduate School of the

University of Colorado in partial fulfillment

of the requirements for the degree of

Master of Science

Department of Electrical, Computer and Energy Engineering

2011

This thesis entitled:
Reverse Link Analysis and Modeling of CDMA based Distributed Antenna Systems
written by Blaze Vincent
has been approved for the Department of Electrical, Computer and Energy Engineering

_____

Dr. Kenneth Baker

_____

Dr. Timothy Brown

_____

Dr. Thomas Schwengler

Date _____

The final copy of this thesis has been examined by the signatories, and we find that both the content and the form meet acceptable presentation standards of scholarly work in the above mentioned discipline.

Vincent, Blaze (M.S, Electrical Engineering)

Reverse Link Analysis and Modeling of CDMA based Distributed Antenna Systems

Thesis directed by Prof. Dr. Kenneth Baker

Distributed Antenna Systems (DAS) are gaining widespread popularity in the indoor wireless market. Most of the existing research literature on this subject has focused on comparing the advantages of DAS systems with traditional macro cells. The goal of this thesis is to define a performance platform for CDMA based distributed antenna systems which can serve as essential design guidelines for future DAS deployments.

One of the major issues presented by DAS systems is the noise floor rise in the reverse link caused by the DAS noise figure. This noise rise becomes a limiting factor in determining capacity and coverage of the DAS based network. The common practice of adding an attenuator (padding) in front of the Base Station receiver can bring down the noise floor, but at the same time force the mobile units to transmit at higher power. We establish an operating platform for the DAS so that the system can be effectively operated within the limits of mobile transmit power and base station receive power, maximizing the system capacity.

Dedication

To my family, whose love and support sustained me this far.

Acknowledgements

I would like to thank God for His unfathomable grace and faithfulness, especially in my studies.

I express my sincere gratitude to Prof. Ken Baker for his continual guidance, constructive criticism and father-like support and help all throughout the course of this thesis. I would like to thank Evolutionary Communications Consultants LLC for providing the necessary funding to execute this project well.

I thank my thesis committee members Prof. Tim Brown and Prof. Thomas Schwengler for this guidance and support. I express my gratitude to Doug Kwiatkowski of Verizon Wireless, Ray Fought and Robin Young of Tyco Electronics and Mike Moran of Extreme Engineering for their immense help during the project execution.

Finally, I thank my wife Bhavya for her constant love, care and support as well as my parents for their encouragement and prayers all along this exciting journey.

Contents

Chapter

Tables

Table

Figures

Figure

Chapter 1

Introduction

1.1 Overview

From the dawn of time, man has realized the importance of communication. The variety of communication methods that he has developed range from ancient symbols engraved in cave paintings, smoke signals, carrier pigeons and semaphores to modern inventions such as smart phones and the Internet. Wireless communications has gained increased focus in the 21st century by the proliferation and popularity of mobile phones and hand held devices.

The invention of the electric Telegraph in 1844 marked the beginning of modern communication based on electricity. During the latter half of the 19th century, when telegraph wires were strung across the continents and ocean floors, communication became faster than it has ever been. The unification of electricity and magnetism by James Clark Maxwell in 1864 and the discovery of radio waves by Heinrich Hertz around 1888 enabled wireless telegraphy. This was first commercially realized by Guglielmo Marconi when he sent and received his first radio signals in 1896. Later inventions of vacuum tube amplifiers and the discovery of the ionosphere resulted in extensive use of radio waves in communication during the first half of the 20th century.

A major beneficiary of the miniaturization of electronics, caused by the development of transistors in 1947 and integrated circuits in 1958, was wireless communications. In 1969, Bell Labs introduced the concept of cellular telephony and the first commercial cellular phone network began operations in Japan by the Nippon Telephone and Telegraph (NTT) in 1979. The first generation cellular phone system known as Advanced Mobile Phone System (AMPS) began operations in

1983 in the USA which was soon followed by a 2nd generation digital system known as Global System for Mobile (GSM) in 1991 in Europe. Growing numbers of users and increasing bandwidth requirements led to 3rd generation systems based on Code Division Multiple Access (CDMA) in the early 2000s and Orthogonal Frequency Division Multiplexing (OFDM) based Long Term Evolution (LTE) systems in 2011 [1].

The number of mobile subscribers has steadily grown since its introduction. From Figure 1.1, we can see that it has increased from 739 million in 2000 to 5370 million in 2010 [1] . It can also be noticed that the number of landline subscribers has consistently dwindled since 2005.

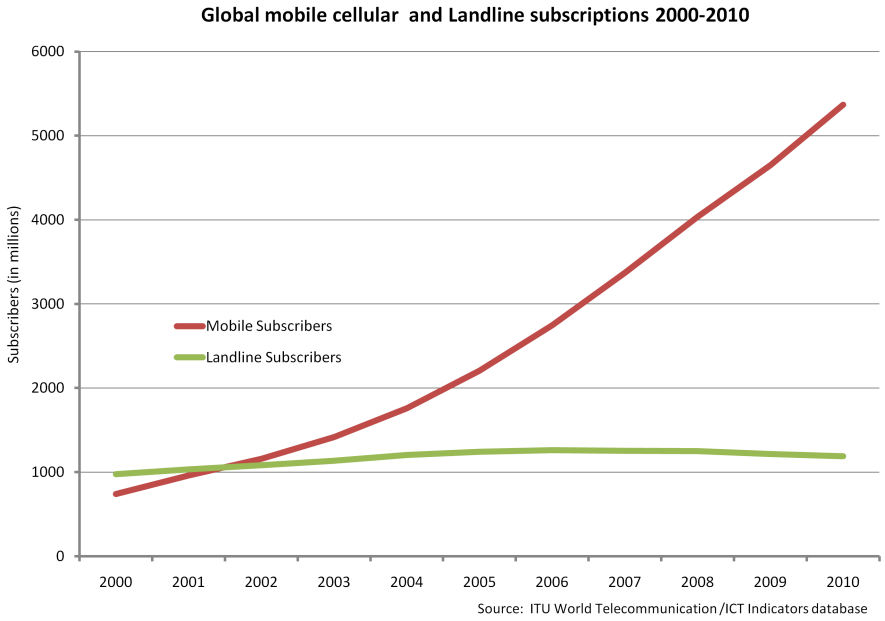

Figure 1.1: Cellular Subscriber statistics from 2000 to 2010

Globally, as of June 2011, GSM has about 76% of the total mobile subscribers while CDMA has about 10%. The complete break down of subscribers with respect to technology is given in figure 1.2[2] . However, CDMA is leading the North American Market with over 50% of the

[1] ITU Statistics: http://www.itu.int/ITU-D/ict/statistics/
[2] www.4gamericas.org

subscribers followed by WCDMA[3] .

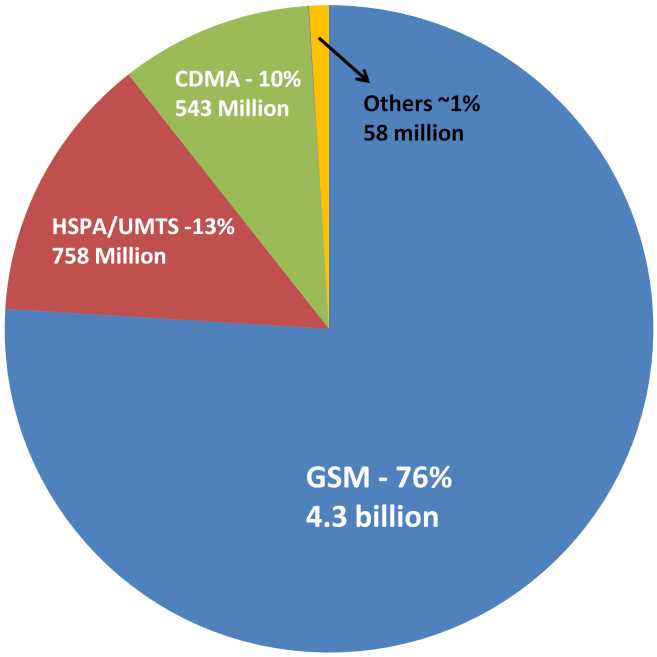

Figure 1.2: Global Cellular Subscribers classified according to Technology - June 2011

As the subscribers grew in number, the service providers identified certain trends in cellular usage. One of the surprising findings was that more than 50% of the traffic was generated indoors. This resulted in the development of various technologies such as radio repeaters, femtocells, picocells and distributed antenna systems to increase the coverage and quality inside buildings. As descirbed in following section, distributed antenna systems have grown to be the best among the variety of indoor solutions proposed. Prior to this discussion, the significance of CDMA based systems in current industry is outlined in the following section.

1.1.1 Market Share, Trends and the Future of CDMA

Although spread spectrum systems have been extensively used in military communication systems from World War II, they were adopted in civilian cellular communication systems only by the late eighties. A prototype system based on Code Division Multiple Access (CDMA), which is

[3] www.cellular-news.com

a modulation and multiple access scheme based on Direct Sequence Spread Spectrum (DSSS), was first demonstrated successfully in 1989 by Qualcomm Inc. in San Diego, California. Inspired by the success of these experiments, a cellular Air Interface Standard was formalized by the Telecommunications Industry Association (TIA) known as EIA/TIA/IS-95A in 1993 for Cellular band and later in 1995 for PCS band (known as ANSI J-STD-008). The first launch of commercial CDMA services was in 1996 in South Korea and the USA. By December 1996, there were more than one million customers worldwide[4] .

The IS-95B standard, which supported 64 kbps data transmissions, a considerable increase over IS-95A, was completed in 1997 and was commercially launched in South Korea in the following year. By 1998, TIA proposed wideband CDMA known as CDMA2000 as a third generation standard and ITU-R selected CDMA2000 1x as the IMT-2000 CDMA standard for 3G services. The ITU-R recognized CDMA2000 1x EV-DO as a part of the IMT-2000 standard in 2001 and the world's first EV-DO network was launched in South Korea in 2002. In April of that year, the 3GPP2 approved CDMA2000 1xEV-DO(Rev A) specification and in March of 2006, the EIA/TIA published CDMA2000 EV-DO(Rev B) standard. It is evident from Figure 1.3 that CDMA customers have steadily grown from 1997 to 2010[5] .

As of August 2011, more than 346 operators in 126 countries offer CDMA2000 services. It currently has 575 million users and accounts for 45% of the 3G market worldwide. CDMA2000 is currently supported in more than 2800 devices marketed by 241 manufacturers. About 127 million of the CDMA2000 subscribers use EV-DO devices and services and its adoption is accelerating at an annual rate of nearly 27% [2]. These numbers underline the significance of better research and analysis that needs to be done for CDMA based networks and their deployment.

[4] CDMA History: http://www.cdg.org/resources/cdma_history.asp
[5] CDG CDMA Subscriber Report, 2010: available http://www.cdg.org

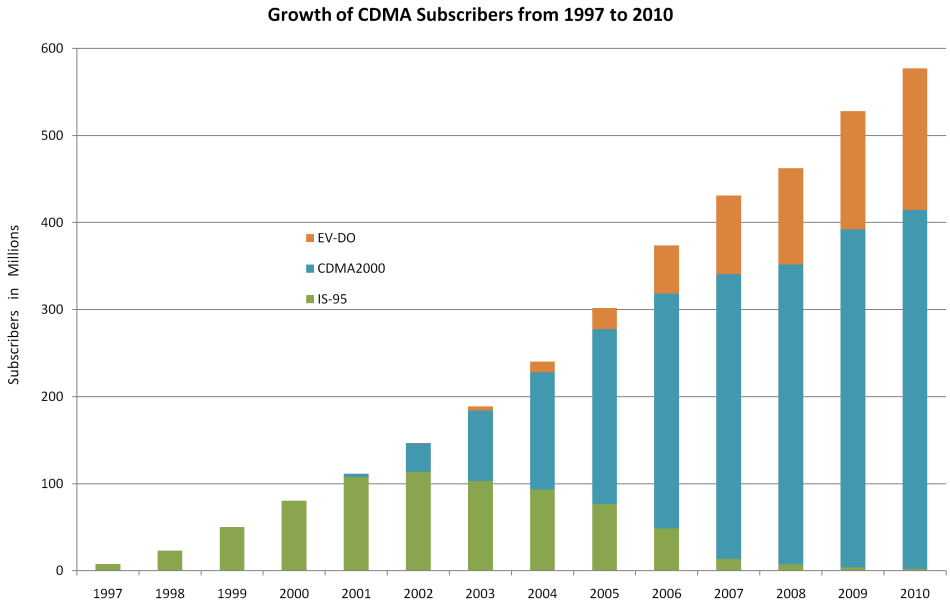

Figure 1.3: Growth of CDMA Subscribers from 1997 to 2010

1.1.2 Market Share, Trends and the Future of DAS systems

The recent analysis in mobile traffic trends shows that over 60% of voice traffic and 90% of data traffic arises from indoors [3]. Indoor coverage is one of the major issues that service providers are facing today. Traditional cellular network design was based on the macrocell concept with an outdoor-in approach where the service provider tried to penetrate buildings from an outside macrocell. Lately, this approach is not providing adequate results because of the energy efficient design and materials used in modern building design. Hence, several indoor coverage solutions such as repeaters, Distributed Antenna systems (DAS), femtocells, picocells as well as WiFi (IEEE 802.11) networks have been developed which can be deployed inside the buildings and can provide better quality and coverage[4].

The concept of Distributed Antenna Systems (DAS) was introduced by Saleh et al. in 1987 as a solution for better indoor coverage using leaky coax cable to simulcast the RF signal[5]. Essentially, DAS is a network of small antennas separated over a geographic area connected back to a head end, which is usually a base station. After their introduction, DAS systems gained

widespread popularity. As of 2008, 96% of inbuilding systems were either active or passive DAS Systems. They have an overall market value of $5.5 billion which is expected to grow up to $15.4 billion in 2014. While other indoor solutions such as femtocells, picocells and WiFi offloading are gaining popularity, DAS remains the primary indoor infrastructure at present [6].

In the light of the above discussion stating the significance of CDMA and DAS systems, the need for a theoretical framework for designing DAS systems is clear. In this thesis, we define a performance platform for CDMA2000 based DAS systems and identify its advantages and limitations.

1.2 Objective of the Thesis

A great deal of research has been done in analyzing and improving the capacity of CDMA based wireless networks and most of them have focused on outdoor macro environments. Much research literature is available on the advantages of DAS systems over traditional single antenna cellular systems. Even though it is an obvious fact that connecting a DAS front end to a base station will considerably increase the reverse link noise floor, its effect on the overall capacity and coverage has been seldom analyzed. The causes and effects of reverse link noise rise and associated impact on capacity is studied, quantified and results are experimentally established in the following chapters of this thesis.

1.2.1 Problem Statement

A Base Station connected to a Distributed Antenna System runs out of capacity on the reverse link before it runs out of capacity on the forward link. This problem has to be studied to identify the impact of DAS on CDMA capacity and a performance platform has to be quantitatively established.

1.3 Overview and Outline of Thesis

The 1st chapter outlines the history and trends in wireless communications and identifies the significance of indoor systems in modern cellular industry. The share of distributed antenna systems in indoor network infrastructure and the need for better DAS design guidelines is evident. This chapter also describes the thesis problem statement and serves as a motivation for contents of following chapters.

The 2nd and 3rd chapters briefly discuss various aspects of CDMA networks and DAS systems. A comprehensive literature survey and important results of recent research done in CDMA capacity and DAS systems is presented. Noise figure, which is an important characteristic of DAS systems, is quantitatively described in chapter 3.

Chapter 4 presents the performance platform of CDMA DAS systems and derives the expressions relating system capacity and coverage to noise and interference. Several numerical results and associated graphs are presented, which can be effectively used as DAS design guidelines. It is shown that system capacity is inversely related to the size of the DAS as well as the number of users it supports.

Chapter 5 outlines the details of various measurements conducted on a large indoor CDMA based DAS system to identify the DAS behavior in varying amounts of traffic. Major results and observations from the data analysis are presented in chapter 6.

Chapter 7 concludes the thesis with major findings and pointers for further analysis and research.

Chapter 2

CDMA Systems

Code Division Multiple Access (CDMA) is a novel channel access method which enables multiple users to access the same radio frequency channel simultaneously by using mutually orthogonal spreading codes to distinguish between themselves. This is in contrast to the other multiple access methods such as Frequency Division Multiple Access (FDMA), in which channels of different frequencies are assigned to different users and Time Division Multiple Access (TDMA), in which the same channel is assigned to different users at different time slots. Simultaneous usage of the same frequency enables CDMA systems to have a frequency re-use factor of 1 and requires less power to be transmitted by the user, enabling the system to have comparatively higher capacity. CDMA is used in the air interface of digital cellular standards IS-95, CDMA2000 as well as WCDMA.

In this chapter, we briefly outline the various aspects of CDMA systems, only in a level of detail required to understand the materials of following chapters. The chapter concludes with a literature survey of research papers about CDMA and CDMA capacity.

2.1 Overview of a CDMA System

Any communication system, including the CDMA system, consists of a transmit stage, a channel, a receive stage and link management as represented in Figure 2.1. In this section, we briefly look at the functionalities of the various blocks shown and how they are implemented in a CDMA system.

Mobile cellular systems are duplex, in which information is simultaneously exchanged in both

directions, namely the forward link (from the base station to the mobile station) and the reverse link (from the mobile back to the base station). CDMA systems use Frequency Division Duplex (FDD) channels, in which separate frequencies are used for forward and reverse links. Figure 2.1 applies equally to both directions but the information characteristics and channel parameters vary significantly from one to the other. For a detailed treatment of the subject, refer to [7].

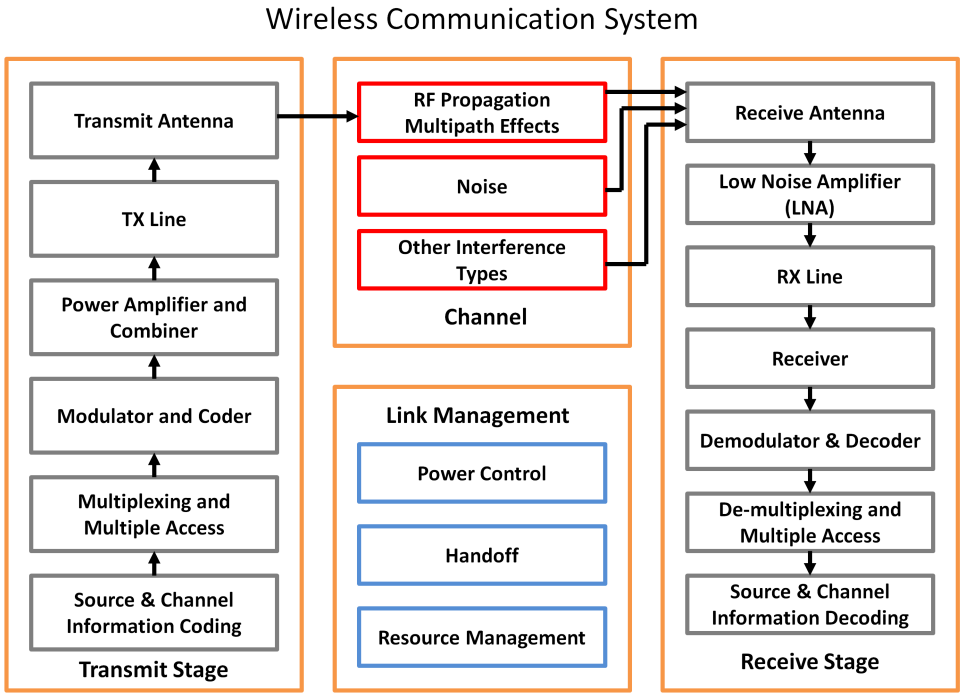

Figure 2.1: Blocks of a Communication System

2.1.1 Transmit Stage

In the transmit stage, the information to be transmitted, which is either voice or data, is encoded, multiplexed, prepared for multiple access, modulated and finally sent to the air as electromagnetic waves. The voice information is analog and is efficiently digitized using vocoders. Both digitized voice and data information are encoded using error detection codes to ensure the integrity of the messages. In order to combat the errors caused by the Rayleigh fading channel, CDMA systems use a class of Forward Error Correction (FEC) codes known as convolutional codes.

The coded signal is also interleaved to avoid blocks of contiguous errors.

Since multiple users have to use the system simultaneously, the system has to make sure that individual information of the users is not lost and privacy and security is maintained. Orthogonal codes are used to spread the individual user signals in order to isolate between them. The receiver stage can extract the signal pertaining to its user by using a copy of the original orthogonal code specific to it. Two types of codes used in CDMA systems are Walsh Codes, which are orthogonal codes generated from the Hadamard Matrix, and PN (Pseudo Noise) Codes, which are semi-orthogonal codes generated using linear feedback shift registers. On the forward link, the Walsh codes are used to identify each user signal, and on the reverse link, they are used as a symbol alphabet. Any PN code has zero cross-correlation with any shifted version of itself. PN codes of two different lengths, namely Short Codes (used to identify the cell sector) and Long Codes (used for privacy and encryption), are used in CDMA systems.

After the source information is encoded and multiplexed, it is modulated to an RF carrier for transmission. CDMA systems use several modulation schemes such as Quadrature Phase Shift Keying (QPSK) and various levels of Quadrature Amplitude Modulation (QAM). Finally the modulated RF signal is fed to an antenna and gets transmitted over the channel.

To summarize, the forward link signal waveform is constructed by combining together several convolutionally encoded user information signals, each of them bi-phase modulated with a user specific Walsh code for user identification and then bi-phase modulated again using a user specific long PN Code for ensuring privacy. This combined waveform is finally quadri-phase modulated with two mutually orthogonal sector specific short PN codes, centered around the assigned channel frequency. The simplified forward link architecture is represented in the Figure 2.2 below.

Unlink the forward link, the reverse link signal waveform is constructed by initially encoding the user information using convolutional encoding and then bi-phase modulated with information dependent Walsh code in order to achieve very low bit errors. It is then bi-phase modulated using user specific long PN Code for privacy. Finally, it is quadri-phase modulated using a sector specific quadrature pair of short PN codes. A simplified block diagram of reverse link architecture is shown

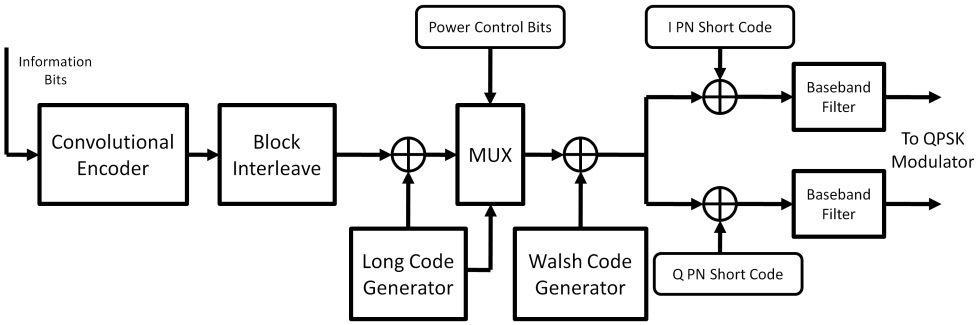

Figure 2.2: Simplified Forward Link Architecture Block Diagram

in figure 2.3 below [8, 9, 10].

Different types of channels exist in the forward and the reverse directions, serving different purposes. In IS-95 systems, the forward link consists of several types of channels, namely **the pilot channel**, which simply carries the quadrature pair of PN short codes specific to the sector, **the synchronization channel**, which carries important information such as system ID, network ID, system time, and one or more **paging channels**, which inform the users about incoming calls and to aid in call setup. There are also the traffic channels which carry user specific information. Similarly, the reverse link consists of traffic channels and access channels. CDMA2000 systems have several additional channels such as the reverse link pilot channels and control channels besides traffic and access channels, providing higher functionality.

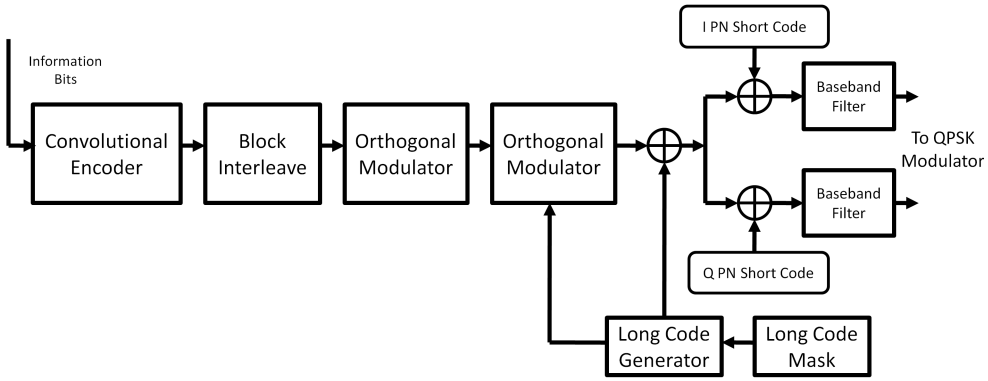

Figure 2.3: Simplified Reverse Link Architecture Block Diagram

The Base Station transmit stage consists of a power amplifier and combiner unit on the

forward link to combine signals of various users and amplify it before transmission. Combined signals are then fed to the antenna using an RF transmission line with proper impedance matching to achieve minimum reflection and loss.

2.1.2 Channel

Channel is that part of the system through which the signal from transmit antenna is propagated through to the receiver. Channel is the most complex and less predictable part of any wireless communication system. In real life, RF propagation is extremely complex and difficult to predict. Distributed Antenna Systems are one of the many ways by which uncertainties of the channel behavior can be reduced.

The signal encounters various changes in the course of its travel. These propagation effects can be classified into large scale fading (also known as propagation loss) and small scale fading. Signal energy from the transmitter is launched in all directions defined by the antenna radiation pattern, and as a result, only a small portion of it reaches the receiver. This is known as propagation loss and the ratio of received power with respect to transmitted power depends on the distance between transmitter and receiver. It can be characterized by the path loss exponent. Due to the various inhomogeneities along the path, the received signal is not always exactly as predicted by the propagation loss, but the variations statistically follow a log normal distribution (a phenomena is known as shadowing)[11]. As the signal propagates, it gets reflected by various objects along the path such as buildings, the ground and foliage in addition to being phase shifted. As a result, multiple copies of the same signal reaches the receiver and causes constructive and destructive interference. This phenomenon, caused by multi-path signals, is known as small scale fading. Small scale fading is also caused by moving objects along the path which introduces a shift in frequency of the signal, known as Doppler spread. Several empirical and physical models have been developed to correctly predict the received signal strength for various channel conditions [12, 13, 14, 15].

At the receiver, besides the transmitted signal, noise generated by various sources as well as interference caused by other users are also received. The signal to noise ratio at the receiver should

be large enough to enable the receiver to correctly retrieve the original signal from the combined signal, noise and interference.

2.1.3 Receiver Stage

The signal, mixed with noise and interference, received at the antenna is initially amplified and then filtered to remove the unwanted frequencies. This is then de-multiplexed and demodulated to retrieve the baseband information. In the forward link, the mobile receives signals from various base stations, from which it searches for the strongest signal by comparing the composed signal with different PN Offsets. It then decodes the signal by aligning it with proper Walsh Codes. Finally the decoded signal is de-interleaved and corrected for errors which yields the original baseband information. In the reverse link, the base station separates the signals received from various users using their specific long PN code mask and sends it to a comparator to determine which Walsh code was sent and ultimately retrieve the data stream.

2.1.4 Link Management

The function of the link management is to make sure several links operate simultaneously in the system with the least possible interference from each other. This is achieved using three tools:

Hand-off: Hand-off is the process by which communication with a mobile from one base station is transferred to another base station. This is required when the mobile is moving from the coverage area of one base station to another. Three types of hand-offs are possible: hard hand-off (a break before make mechanism, used when carrier frequency has to be changed when user moves from one cell to another), soft hand-off (a make before make mechanism, used when same frequency is used in both cells involved in hand-off) and softer hand-off (soft hand-off between 2 sectors of the same cell). CDMA systems use soft hand-off since, both cells use the same frequency. The decision of hand-off is made by the base station based on the feedback received from mobile regarding the received pilot signal level. If the level of the pilot signal from current base stations drops of below a certain threshold,

the base station initiates the hand-off procedure to be moved to another base station with higher pilot signal strength.

Power Control: CDMA systems require that all signals from the users are received at the same power level at the base station. It can be seen that by allowing signals to reach the base station at a power level that provides minimum signal to interference ratio, capacity is maximized. If the signal level from the user is too low, the bit error rate will be too high to allow a good quality communication and if the signal is too high, it will cause interference to all other users in the cell. The CDMA systems uses two methods of power control:

Open Loop Power Control: In this method, the user equipment measures the received power level of the pilot channel and uses this level to estimate the required transmit power. This value is then used to calculate the power level to be transmitted which is specifically given by (2.1). p_r represents the power level of the forward pilot channel. -73 dB is the default value chosen for cellular band. For PCS band, the value is -76. NOM_PWR and $INIT\_PWR$ are system parameters used for fine tuning.

$$p_t = -p_r - 73 + NOM\_PWR + INIT\_PWR. \tag{2.1}$$

Closed Loop Power Control: This is a base station assisted process of continuously adjusting the transmit power in order to compensate for fading. In this method, the base station continuously monitors the reverse link quality using an indicator known as Frame Erasure Rate and commands the user to power up or down to maintain an acceptable E_b/N_o. The Base Station sends this instruction to change the transmit power level, which is usually in steps of $+1$ dB or -1 dB, on the forward link in the form of power control bits. The total transmit power can be thus represented as (2.2).

$$p_t = -p_r - 73 + NOM\_PWR + INIT\_PWR + \sum(\text{closed loop corrections}) \tag{2.2}$$

Resource Management: Hand-off and power control are the resource management tools of IS-

95 systems as the main traffic is voice. However, CDMA2000 systems carries both voice and data and provides several advanced features not available in IS-95. Hence, CDMA2000 systems require more complex resource management. The function of resource management is to schedule different data services that have different requirements, according to network availability, to maximize the overall throughput. For example, supplemental channels with higher data rates are dynamically assigned to data calls as required.

It has to be mentioned that the hand-off, power control and resource management functions are not designed, considering distributed antenna systems. DAS systems are capable of making these functions more efficient.

In the following section, we compare and contrast the various CDMA standards that exist in the market.

2.2 Comparison of Different CDMA Standards

The first CDMA standard, called IS-95A, was developed in 1995. It used 1.25 MHz channels with a chip rate of 1.2288 Mcps. Four types of logical channels are used in the forward link: Pilot channel, Synch Channel, Paging Channels and Traffic Channels. Two types of channels are used in the reverse link: Access Channel and Traffic Channels. IS-95 systems employ Frequency Division Duplex (FDD) multiplexing and Binary Phase Shift Keying (BPSK) modulation and can achieve a data-rate of 14.4 Kbps. A revision of the standard called IS-95B was introduced in 1997 which included Supplemental Code channels in both forward and reverse links, in order to increase the data rate up to 114 Kbps.

Demand for a third generation standard resulted in the publication of the CDMA2000 family of standards, the first of which is known as 1xRTT, released in 1999. Parameters such as channel bandwidth, modulation and spreading code length were determined based on Radio Configurations (RC) and Spreading Rates (SR). SR1 systems have channel bandwidth of 1.25 MHz while systems with SR3 had 3 simultaneous 1.25 MHz channels on the forward link and 1 3.75MHz channel on the

reverse link. The former systems are called 1x systems, while the latter are known as 3x systems. Based on the Radio Configuration, CDMA2000 systems had modulation schemes such as BPSK, QPSK,8-PSK or 16-QAM as well as Walsh Code lengths ranging from 4 to 128. There are 10 types of logical channels on the forward link and 5 types of logical channels on the reverse link.

In order to support data services, another family of standards known as CDMA2000 Evolution Data Optimized (EV-DO) were introduced. EV-DO Release 0 was introduced in 2001, Revision A in 2004 and Revision B in 2006 respectively. EV-DO systems employ 4 types of forward link channels and 4 types of reverse link channels and can achieve data rates of 4.9 Mbps. Networks employing EV-DO are end-to-end packet switched,while those employing CDMA2000 1x are circuit switched networks.

In this thesis, we focus our attention on CDMA2000 1xRTT based network.

2.3 CDMA Capacity

The quality of a communication link can be characterized by bit error rate (BER), which is defined as the probability that a transmitted bit is received in error by the receiver. Bit error rate depends on various factors such as the modulation scheme and channel characteristics. BER can be mathematically modeled in terms of the ratio of Energy per bit to Noise spectral density, represented as E_b/N_o [16]. For example, the probability of error of a single bit of information transmitted through an additive White Gaussian Noise (AWGN) Channel using BPSK or QPSK modulation is given by (2.3).

$$P_b = \frac{1}{2}\mathbf{Q}\left(\sqrt{\frac{E_b}{N_o}}\right) \tag{2.3}$$

where $\mathbf{Q}(x)$ is the complementary error function [1] . Typical mobile communication channels are Rayleigh fading channels and not AWGN channels. Moreover, channel coding schemes, which reduce the E_b/N_o requirement for a fixed BER, are used to improve the error performance [10].

Capacity of a cellular system can be defined in various ways as described below.

[1] Definition: http://cnx.org/content/m11537/latest/

Erlang Traffic Capacity: Capacity can be defined as the measure of the traffic load that can be supported by the system for a given quality and availability of service. The traffic load represented in terms of the number of users requesting service that results in a target blocking probability is known as Erlang capacity. Capacity in Erlang is a dimensionless number representing the product of the number of users requesting access to the system (users/time) and average holding time of the user (time/user). It is traditionally used to characterize the traffic of voice systems.

Shannon Channel Capacity: The channel capacity theory developed by C. E. Shannon in 1948 provides a method for calculating the maximum amount of information that can be carried through a channel. Shannon stated that there exists a maximum rate of information C (bits/sec) known as channel capacity for any given communication system and if the information rate R (bits/sec) from a source is less than C, then it can be successfully transmitted over the communication channel with arbitrarily small error probability using intelligent Coding techniques. The maximum capacity of a band limited Gaussian channel operating in the presence of Additive White Gaussian Noise (AWGN) is given by

$$C = B \log_2(1 + \frac{S}{N}) \tag{2.4}$$

where C is the channel capacity, B is the bandwidth in Hz, S is the received power in Watts, N is the average noise power in Watts. $\frac{S}{N}$ is known as the Signal to Noise Ratio (SNR). This equation is applicable to any communication channel and any information type (analog or digital). The ultimate goal of communication research is to achieve the maximum theoretical capacity predicted by Shannon's theory. Efficient coding schemes are developed to achieve this goal.

Even though Shannon capacity is useful in identifying the maximum possible capacity of a channel and the minimum signal to noise ratio requirements for specific data rates in a band limited channel, it is not easy to apply to multi user situations and cellular systems where there is frequency re-use and co-channel interference issues.

User Capacity: User capacity of a CDMA system can be defined as the maximum number of simultaneous users that can be supported by the system while the service quality requirements of the user such as data rate, bit error rate and outage probability are being satisfied[17]. This is a useful measure and is widely used in practical cellular system design. The user capacity of a CDMA system is discussed in detail in chapter 4.

2.4 Literature Review

The CDMA standards are published jointly by the Telecommunications Industry Association and Electronic Industries association. The IS-95A standard for the cellular band was published in 1993[18] and later for the PCS band in 1995 (known as ANSI J-STD-008). CDMA2000 standard was published in 1999[19] and later the EV-DO Release 0[20], Revision A [21] and Revision B [22] in 2001, 2004 and 2006 respectively.

CDMA capacity has been a very interesting research topic and a great deal of literature has been published considering various aspects. Gilhousen et al. published the capacity equation for voice only CDMA systems in [23]. This result is later expanded in [24] by Paulrajan et al. to include multiple classes of users with different bandwidths and different fidelity requirements in a single cell environment. [24] also introduced the concept of capacity plane to visualize the capacity. Optimizing the capacity of multimedia CDMA systems by power control and rate selection has been investigated in [25]. Results of [25] and [24] are combined in [26] to derive the capacity plane of multimedia CDMA services.

The capacity information of a system can be used for Call Admission Control (CAC), by which a user can be allowed or denied access based on the available system resources and the requirements of the user requesting access. It can also be used for resource management, by which if the current users do not use the available system capacity, remaining resources can be allocated to current users to increase system throughput or quality until a new user requests service.

Viterbi and Viterbi analyzed the Erlang capacity of a voice only CDMA system in [27], which was extended by Sampath et al. for integrated voice and data communication[28]. Erlang capacity

is further analyzed for a limited number of channel elements in [29], for multiple sectors and multiple frequency allocation bands in [30], for delay constraint in [31] and for optimized sectoring in [32].

The effect of soft hand-off on CDMA capacity is investigated in [33] and the effect of multi-path fading environment is analyzed in [34]. Capacity enhancements by traffic based control of speech bit rates are described in [35] and by beam forming in [36].

Chapter 3

DAS Systems

3.1 Introduction

The DAS forum[1] defines a Distributed Antenna System as follows:

> A Distributed Antenna System (DAS) is a network of spatially-separated antenna nodes connected to a common source via a transport medium that provides wireless service within a geographic area or structure. DAS antenna elevations are generally at or below the clutter level and node installations are compact.

DAS systems are used both in outdoor environments such as highways, urban areas, subways, tunnels and university campuses as well as indoor environments such as corporate offices, stadiums, complexes, airports, convention centers, hospitals and hotels where a macro site cannot provide better coverage due to the difficult geographical spread as well as the reflections and attenuations from walls, roofs and windows.

DAS systems can be classified into:

Passive vs Active Systems: Passive systems are smaller DAS systems consisting of fewer antenna nodes and without any active components such as amplifiers or gain controllers, while active systems are larger DAS systems that contain amplifiers to compensate for losses. It is more complex to design active systems due to problems such as inter-modulation and distortion.

[1] http://thedasforum.org/

Neutral vs Dedicated Systems: Neutral Host DAS systems are designed to simultaneously serve multiple wireless service providers. As such they will support most of the common cellular technologies such as GSM, CDMA, HSPA, LTE, WiFi and public safety for all common frequency bands such as 700 MHz, 800 MHz, 850 MHz, 1800 MHz, 1900 MHz, 2100 MHz and 2.4 GHz. Dedicated systems normally a single service provider and support only a particular technology in a particular band.

3.2 General DAS Architecture

As shown in the figure 3.1, a DAS system consists of three parts:

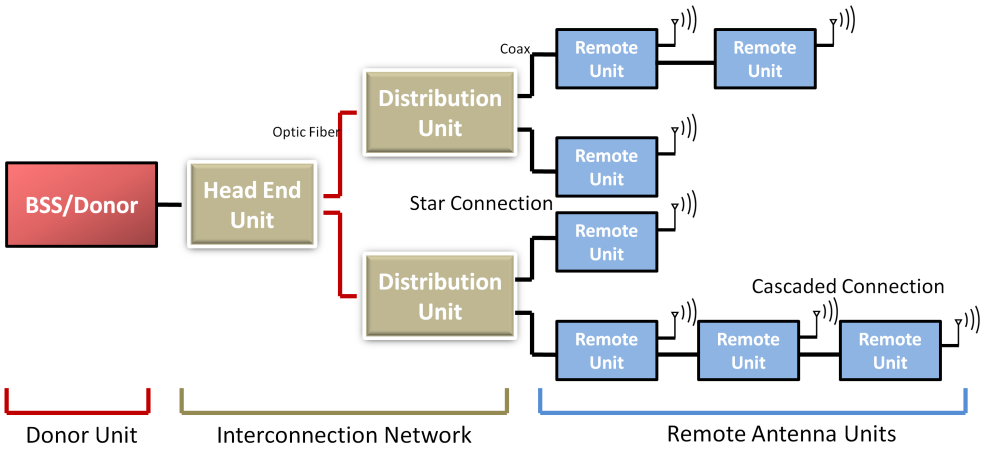

Figure 3.1: General DAS System Architecture

Donor Unit: The donor is normally a base station or a repeater. The repeater will have an external antenna which brings in the forward link signals from the larger cellular network to the DAS unit and takes out the reverse link signal from the DAS unit. One or more donor units typically feed a DAS system.

Remote Unit: Remote units are the antenna nodes that are spread throughout in space. They transmit the forward link signals as electromagnetic waves and receive the reverse link signals to be sent back to the base station.

Interconnection Network: Donor units and remote units are connected to each other by the interconnection network. It will normally have a head end unit and one or more distribution units. The interconnection network can be built either by using only passive components such as splitters, combiners and cables, or can include active components such as bi-directional amplifiers and automatic gain controllers. The remote units can be either star-connected to the distribution unit or cascaded. Either of the below methods are generally used as interconnection media:

(1) Standard **Coaxial Cables** that carry RF signals are generally used to connect the distribution units to the remote antenna units.

(2) Single mode and multi mode **Optic Fibers** with necessary components such as splitters and multiplexers are generally used to connect the head end to the distribution units.

(3) Larger DAS systems have both optical fibers and coaxial cables and are generally known as the **Hybrid Fiber Cable (HFC)** network.

(4) For outdoor DAS units, especially those deployed along highways and tunnels, **over-the-air repeaters** are used, which receive and transmit the signals from the donor and pass it to the remote units over the air as electromagnetic waves.

3.3 Advantages of DAS Systems

The goal of an RF distribution system is to distribute the RF signal uniformly throughout the coverage area. It has been proved that distributed antenna systems achieve this goal very well.

The major difficulty faced in indoor environments is the path loss, which is caused by shadowing due to the presence of walls, objects like ceilings and multi-path fading, which is caused by signal reflections. Since the multi-path signals arrive more quickly in indoor environments, the RMS delay spread is much smaller than the symbol period and results in flat fading. Even though CDMA systems can utilize multi-paths for their benefit with the use of Rake receivers, it is not

possible to resolve individual multi-path signals, which causes flat fading.

Distributed antenna systems are shown to overcome both of the above mentioned issues along with several other advantages. Some of them are listed below [37]. For the below discussion, consider the general path loss model given by (3.1). The path loss, defined as the ratio of transmitted power to received power, is given by:

$$\text{Path Loss} = \frac{P_T}{P_R} = C.R^{\nu} \tag{3.1}$$

where:

P_T the transmitted power (Watts)

P_R the received power at a distance R (Watts)

C the path loss at a reference distance of 1m (Watts)

ν the path loss exponent

Maximizing Coverage Area: For a given transmit power, distributed antenna systems can cover more geographical area than single antenna systems. Assuming omni-directional antennas, an N element distributed antenna system (and assuming the transmit power is equally divided between them) can improve the coverage over a single antenna system by a factor of:

$$\text{Coverage improvement factor:} \quad N^{1-\frac{2}{\nu}} \tag{3.2}$$

Minimizing Radiated Power: For a given coverage area, distributed antenna systems require less power to be transmitted by the base station and the mobiles. Again, assuming omni-directional antennas and same path loss in the forward and reverse directions, an N element DAS will have a power savings in the forward link by a factor given by (3.3) and in the reverse link by a factor given by (3.4). It is experimentally shown that mobile transmit power is reduced by 10 dB in a DAS system compared to a single antenna [38]. This will result in a direct capacity improvement.

$$\text{Forward link power reduction factor:} \quad N^{1-\frac{\nu}{2}} \tag{3.3}$$

$$\text{Reverse link power reduction factor:} \quad N^{-\frac{\nu}{2}} \tag{3.4}$$

Path and Time diversity: DAS systems offer path diversity since a mobile can communicate to several remote antenna units simultaneously. It has been suggested that by including delay elements between the antenna nodes, the delay spread can be increased to cause frequency selective fading. Both of these are advantageous to CDMA systems because of the capabilities of the Rake receiver. Multiple copies of the signal can be combined at the receiver using several techniques such as Maximal Ratio Combining (MRC), Equal Gain Combining (EGC) or Selection Combining (SC), thereby increasing the received signal-to-noise ratio [39]. It has to be noted that multiple antennas also can cause self interference and performance degradation. The path diversity-self interference trade off has to be taken into account while designing a DAS System [40].

Higher Spectral Efficiency: Distributed antenna systems reduce the far field interference when compared to a single antenna system. This results in better spectral efficiency [41].

3.4 The noise figure of a DAS

Noise figure is a measure of the degradation of the signal-to-noise ratio (SNR), as the signal passes through the network. Every practical network adds some extra noise from its various components to the signal, thereby degrading the overall SNR. Thus noise figure is an important parameter which characterize the network performance. It is formally defined as the ratio of the input signal-to-noise ratio to the output signal-to-noise ratio available at the device terminals [42]. In other words, a device would raise the output noise floor by an amount equal to its noise figure.

The thermal noise generated by a load is given by (3.5)

$$N = k \cdot T \cdot B \tag{3.5}$$

where k is Boltzmann's constant, equal to $1.38 \cdot 10^{-23} J/K$, T is the absolute temperature in Kelvin, and B is the measurement bandwidth.

The noise figure quantifies the total amount of noise in terms of the noise that would remain if the device itself did not introduce any noise. It is thus the ratio of the total output noise to the input thermal noise at a standard temperature of 290 K. It is usually represented in decibels as defined in the equation (3.6).

$$\text{Noise Figure} = 10 \cdot \log\left(\frac{S_i/N_i}{S_o/N_o}\right) = \frac{SNR_{in}}{SNR_{out}} \tag{3.6}$$

The major impact of a DAS system on the cellular network is its noise contribution. The variations in the noise contribution depend on several factors such as number of antenna nodes, their interconnection strategy and the overall DAS layout. This area is less explored in DAS literature and will be the main area of concentration of this thesis. Here we derive expressions for the noise figure of various DAS topologies, seen by the mobile stations. These results are utilized in further chapters.

As mentioned in the previous section DAS systems are generally either star connected or cascaded, the former being most common. We consider both models, initially with 2 antenna elements and then with N elements connected to the head-end unit as shown in figure 3.2

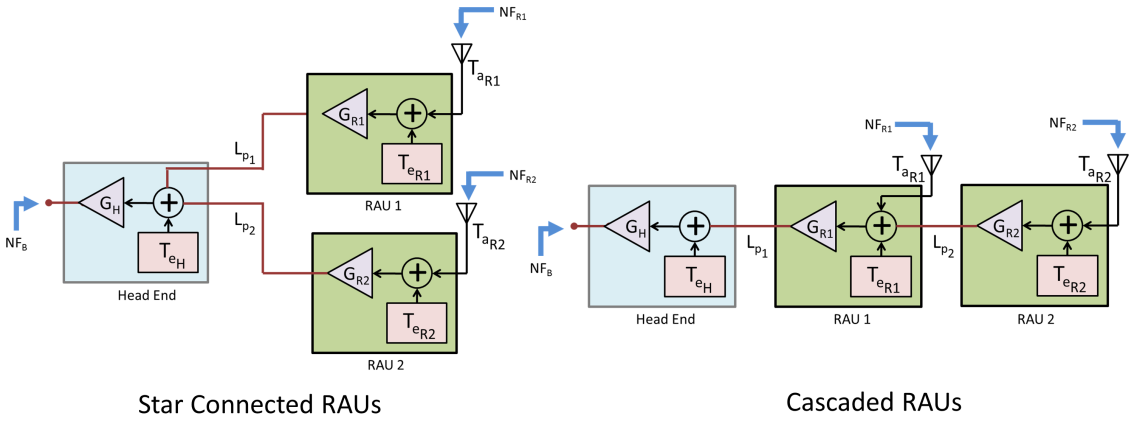

Figure 3.2: Star-connected and Cascaded DAS with two Antenna elements

We define the variables shown in the Figure 3.2 as below:

NF_{R1}, NF_{R2} : effective noise figure of the DAS, felt by the mobile station connected to

RAU-1 and RAU-2 respectively

$T_{a_{R1}}, T_{a_{R2}}$: antenna temperature of RAU-1 and RAU-2 respectively

$T_{e_{R1}}, T_{e_{R2}}$: equivalent noise temperature of the RAUs

G_{R1}, G_{R2} : gain of the RAUs. For passive RAUs, it is approximately 1 (0 dB)

T_{e_H} : equivalent noise temperature of the head end unit

G_H : gain of the head end unit. It is 1 for passive DAS systems and greater than 1 for active systems

L_{p_1}, L_{p_2} : losses incurred by the cables connecting the RAUs to the head end. They are characterized in terms of the cable length.

N_{R2} : nominal noise figure of RAU-2

N_{R1} : nominal noise figure of RAU-1

N_H : nominal noise figure of the head end

Now,

$G_{T1} = G_{R1} \cdot L_{P_1}$

$G_{T2} = G_{R2} \cdot L_{P_2}$

Case 1:NF_{R1} of Star Connected DAS

$$NF_{R1} = N_{R1} + N_{R2} \cdot \frac{G_{T2}}{G_{T1}} + \frac{N_H}{G_{T1}} \tag{3.7}$$

Proof:

Input Signal = S_i

Input Noise Density = $k \cdot T_{a_{R1}}$

Output Signal = $S_i \cdot G_{R1} \cdot G_H \cdot L_{P_1}$

Output Noise Density = $k \cdot G_H[(T_{a_{R1}} + T_{e_{R1}}) \cdot G_{T1} + (T_{a_{R2}} + T_{e_{R2}}) \cdot G_{T2} + (T_{a_H} + T_{e_H})]$

Effective Noise Figure =

$$NF_{R1} = \frac{S_i/k \cdot T_{a_{R1}}}{S_i \cdot G_{R1} \cdot G_H \cdot L_{P_1}/k \cdot G_H[(T_{a_{R1}} + T_{e_{R1}}) \cdot G_{T1} + (T_{a_{R2}} + T_{e_{R2}}) \cdot G_{T2} + (T_{a_H} + T_{e_H})]}$$

$$= \frac{S_i \cdot k \cdot G_H[(T_{a_{R1}} + T_{e_{R1}}) \cdot G_{T1} + (T_{a_{R2}} + T_{e_{R2}}) \cdot G_{T2} + (T_{a_H} + T_{e_H})]}{k \cdot T_{a_{R1}} \cdot S_i \cdot G_H \cdot G_{T1}}$$

$$= \frac{T_{a_{R1}} + T_{e_{R1}}}{T_{a_{R1}}} + \frac{T_{a_{R2}} + T_{e_{R2}}}{T_{a_{R1}}}\left(\frac{G_{T2}}{G_{T1}}\right) + \frac{T_{a_H} + T_{e_H}}{T_{a_{R1}}}\left(\frac{1}{G_{T1}}\right)$$

Let, $T_{a_{R1}} = T_{a_{R2}} = T_{a_H} = T_0 = 290K$

$$\rightarrow NF_{R1} = N_{R1} + N_{R2}\left(\frac{G_{T2}}{G_{T1}}\right) + \frac{N_H}{G_{T1}} \tag{3.8}$$

Case 2: NF_{R2} of Star Connected DAS

$$NF_{R2} = N_{R2} + N_{R1}.\frac{G_{T1}}{G_{T2}} + \frac{N_H}{G_{T2}} \tag{3.9}$$

Proof:

Input Signal = S_i

Input Noise Density = $k \cdot T_{a_{R2}}$

Output Signal = $S_i \cdot G_{R2} \cdot L_{P_2} \cdot G_H$

Output Noise Density = $k \cdot G_H[(T_{a_{R1}} + T_{e_{R1}}) \cdot G_{T1} + (T_{a_{R2}} + T_{e_{R2}}) \cdot G_{T2} + (T_{a_H} + T_{e_H})]$

Effective Noise Figure =

$$NF_{R1} = \frac{S_i/k \cdot T_{a_{R2}}}{S_i \cdot G_{R2} \cdot L_{P_2} \cdot G_H/k \cdot G_H[(T_{a_{R1}} + T_{e_{R1}}) \cdot G_{T1} + (T_{a_{R2}} + T_{e_{R2}}) \cdot G_{T2} + (T_{a_H} + T_{e_H})]}$$

$$= \frac{S_i \cdot k \cdot G_H[(T_{a_{R1}} + T_{e_{R1}}) \cdot G_{T1} + (T_{a_{R2}} + T_{e_{R2}}) \cdot G_{T2} + (T_{a_H} + T_{e_H})]}{k \cdot T_{a_{R2}} \cdot S_i \cdot G_{T2} \cdot G_H}$$

$$= \frac{T_{a_{R2}} + T_{e_{R2}}}{T_{a_{R2}}} + \frac{T_{a_{R1}} + T_{e_{R1}}}{T_{a_{R2}}}\left(\frac{G_{T1}}{G_{T2}}\right) + \frac{T_{a_H} + T_{e_H}}{T_{a_{R2}}}\left(\frac{1}{G_{T2}}\right)$$

Let, $T_{a_{R1}} = T_{a_{R2}} = T_{a_H} = T_0 = 290K$

$$\rightarrow NF_{R2} = N_{R2} + N_{R1}\left(\frac{G_{T1}}{G_{T2}}\right) + \frac{N_H}{G_{T2}} \tag{3.10}$$

Case 3: NF_{R1} of Cascaded DAS

$$NF_{R1} = N_{R1} + N_{R2} \cdot G_{T2} + \frac{N_H}{G_{T1}} \tag{3.11}$$

Proof:

Input Signal = S_i

Input Noise Density = $k \cdot T_{a_{R1}}$

Output Signal = $S_i \cdot G_{R1} \cdot L_{P_1} \cdot G_H$

Output Noise Density = $k \cdot G_H[(T_{a_{R1}} + T_{e_{R1}}) \cdot G_{T1} + (T_{a_{R2}} + T_{e_{R2}}) \cdot G_{T2}G_{T1} + (T_{a_H} + T_{e_H})]$

Effective Noise Figure =

$$\begin{aligned} NF_{R1} &= \frac{S_i/k \cdot T_{a_{R1}}}{S_i \cdot G_{R1} \cdot L_{P_1} \cdot G_H/k \cdot G_H[(T_{a_{R1}} + T_{e_{R1}}) \cdot G_{T1} + (T_{a_{R2}} + T_{e_{R2}}) \cdot G_{T2} \cdot G_{T1} + (T_{a_H} + T_{e_H})]} \\ &= \frac{S_i \cdot k \cdot G_H[(T_{a_{R1}} + T_{e_{R1}}) \cdot G_{T1} + (T_{a_{R2}} + T_{e_{R2}}) \cdot G_{T2} \cdot G_{T1} + (T_{a_H} + T_{e_H})]}{k \cdot T_{a_{R1}} \cdot S_i \cdot G_{T1} \cdot G_H} \\ &= \frac{T_{a_{R2}} + T_{e_{R2}}}{T_{a_{R1}}} \cdot G_{T2} + \frac{T_{a_{R1}} + T_{e_{R1}}}{T_{a_{R1}}} + \frac{T_{a_H} + T_{e_H}}{T_{a_{R1}}}\left(\frac{1}{G_{T1}}\right) \end{aligned}$$

Let, $T_{a_{R1}} = T_{a_{R2}} = T_{a_H} = T_0 = 290K$

$$\rightarrow NF_{R1} = N_{R1} + N_{R2} \cdot G_{T2} + \frac{N_H}{G_{T1}} \tag{3.12}$$

Case 4: NF_{R2} of Cascaded DAS

$$NF_{R2} = N_{R2} + \frac{N_{R1}}{G_{T1}} + \frac{N_H}{G_{T2} \cdot G_{T1}} \tag{3.13}$$

Proof: Input Signal = S_i

Input Noise Density $= k \cdot T_{a_{R2}}$

Output Signal $= S_i \cdot G_{R2} \cdot L_{P_2} \cdot G_{R1} \cdot L_{P_1} \cdot G_H = S_i \cdot G_{T2} \cdot G_{T1} \cdot G_H$

Output Noise Density $=$

$k \cdot G_H[(T_{a_{R1}} + T_{e_{R1}}) \cdot G_{T1} \cdot G_H + (T_{a_{R2}} + T_{e_{R2}}) \cdot G_{T2}G_{T1} + (T_{a_H} + T_{e_H})]$

Effective Noise Figure $=$

$$NF_{R2} = \frac{S_i/k \cdot T_{a_{R2}}}{S_i G_{T2} G_{T1} G_H/k \cdot G_H[(T_{a_{R1}} + T_{e_{R1}}) \cdot G_{T1} \cdot G_H + (T_{a_{R2}} + T_{e_{R2}}) \cdot G_{T2} \cdot G_{T1} + (T_{a_H} + T_{e_H})]}$$

$$= \frac{S_i \cdot k \cdot G_H[(T_{a_{R1}} + T_{e_{R1}}) \cdot G_{T1} \cdot G_H + (T_{a_{R2}} + T_{e_{R2}}) \cdot G_{T2} \cdot G_{T1} + (T_{a_H} + T_{e_H})]}{k \cdot T_{a_{R2}} \cdot S_i \cdot G_{T2} \cdot G_{T1} \cdot G_H}$$

$$= \frac{T_{a_{R2}} + T_{e_{R2}}}{T_{a_{R2}}} + \frac{T_{a_{R1}} + T_{e_{R1}}}{T_{a_{R2}}} \cdot \frac{1}{G_{T2}} + \frac{T_{a_H} + T_{e_H}}{T_{a_{R2}}} \left(\frac{1}{G_{T2} \cdot G_{T1}} \right)$$

Let, $T_{a_{R1}} = T_{a_{R2}} = T_{a_H} = T_0 = 290K$

$$\rightarrow NF_{R2} = N_{R2} + \frac{N_{R1}}{G_{T2}} + \frac{N_H}{G_{T2} \cdot G_{T1}} \tag{3.14}$$

We generalize the above results to the case of N RAUs which are shown in figures 3.3 and 3.4 as follows:

Case 1: NF_{R_i} of Star Connected DAS

$$NF_{R_i} = \frac{1}{G_{T_i}} \cdot \left[N_H + \sum_{k=1}^{n} N_{R_k} \cdot G_{T_k} \right] \qquad \forall i. \tag{3.15}$$

Case 2: NF_{R_i} of Cascaded DAS

$$NF_{R_i} = \frac{N_H}{\left(\prod_{p=1}^{i} G_{T_p} \right)} + \frac{\sum_{k=1}^{i-1} N_{R_k}}{\left(\prod_{p=k+1}^{i} G_{T_p} \right)} + N_{R_i} + \sum_{k=i+1}^{n} N_{R_k} \cdot \left(\prod_{p=i+1}^{k} G_{T_p} \right) \tag{3.16}$$

Active DAS systems are designed in such a way that the end-to-end gain is 1 (0 dB). This implies that $G_{T_k} = 1$. In this case, equations (3.15) and (3.16) are reduced to (3.17).

$$NF_{R_i} = N_H + \sum_{k=1}^{n} N_{R_k} \tag{3.17}$$

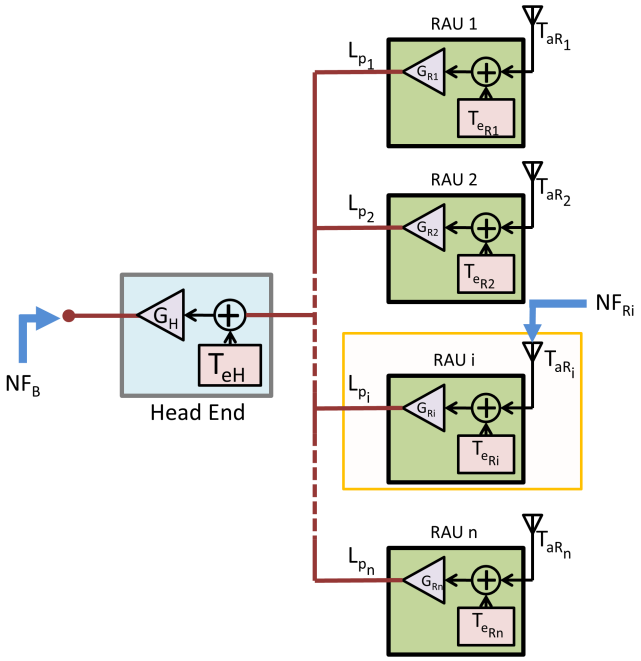

Figure 3.3: Star-connected DAS with n Antenna elements

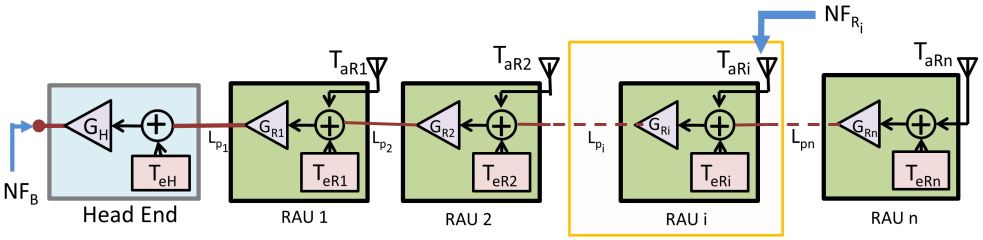

Figure 3.4: Cascaded DAS with n Antenna elements

3.5 Literature Review

Distributed antenna systems, which can be implemented using leaky coaxial cables were proposed by Saleh et al. in 1987 as a solution to fill in the gaps in indoor coverage[5]. Later this idea of simulcasting a signal using a number of antenna units connected to a central base station is adopted into cellular networks[43, 44, 45]. Salamasi proposed distributed antenna systems for CDMA in 1991 knowing the fact that multi-path signals can be used for diversity reception by the

RAKE receivers thereby increasing the capacity [8, 39]. An experimental model of a DAS was built and studied by Xia et al, and established the requirement of diversity-self-interference trade-off in DAS designs [38] which was later mathematically analyzed by [40].

Most of the studies focused on performance analysis and comparison of DAS systems with traditional centralized antenna systems. Several of them were based on mathematical analysis [37, 46, 47] and other on computer simulations [41, 48, 49, 50]. These studies identified the advantages of DAS systems as described in the previous section. The outage probability of DAS systems assuming that CDMA systems are interference limited is mathematically calculated in [51].

Recent development in Multiple Input Multiple Output (MIMO) theory[52] has motivated the analysis of distributed antenna systems with MIMO. [53, 54, 55, 56]. The information theoretic capacity of MIMO DAS systems are treated in [57, 58]. They showed that DAS systems can achieve improved capacity and coverage both in single cell and multi cell situations.

Recent literature focus on the performance of DAS systems over various channel characteristics as well as treating DAS systems with cooperative communication principles [59, 60]. Performance over composite Log Normal and Nagakami-m fading channels is treated in [61], over generalized fading channels in [62] and shadowed fading channels is treated in [63]. The sum link capacity of DAS systems is compared to a co-located antenna system in [64] and downlink performance and channel capacity is treated in [65].

Distributed antenna systems provide significant advantages in capacity, spectral efficiency and power requirements over traditional macro-cellular systems and are extensively used in the indoor cellular systems. Even though research associated with interference analysis is done, noise contributions of DAS systems have not been dealt with. It is this issue to which we focus in this thesis.

Chapter 4

Performance Platform of a CDMA DAS

The existing CDMA literature has different opinions regarding whether CDMA is uplink or downlink limited, noise or interference limited and coverage or capacity limited [66]. Even though it is a common notion that CDMA systems are interference limited in uplink because of the reduction of signal quality with increased simultaneous users, it is subject to several assumptions that are not often stated. Noise is often ignored in several cases, owing to the fact that interference is significantly higher than background noise. However, in a CDMA DAS environment, noise can also become a significant limiting factor in certain cases. This subject is elaborated in the following sections, in which, we attempt to define the performance limits of CDMA DAS and provide some design guidelines which can be used to design large DAS systems effectively.

4.1 System Parameters

In order to model the performance platform for a CDMA DAS, we define the following parameters:

W The channel bandwidth expressed in Hz.

R The traffic channel data rate expressed in bits/seconds (bps). As mentioned in Chapter 2, for IS-95 systems, the rate is either 9.6 kbps or 14.4 kbps and for CDMA2000 systems, it depends on radio configuration and spreading rates.

W/R Processing gain.

S The received signal power. It is usually expressed in Watts or in dBm.

N_o The noise power spectral density which is expressed in Watts/Hz or dBm/Hz.

N The total noise power across the channel bandwidth in Watts or dBm, expressed as $N_o \cdot W$. It is a sum of system and background generated noise as well as user generated interference.

S/N Signal-to-Noise Ratio (SNIR).

E_b Energy per bit.

E_b/N_o The ratio of normalized energy per bit to noise spectral density, which is a fundamental performance criterion of CDMA systems. As mentioned in Chapter 2, the BER can be expressed in terms of E_b/N_o for each modulation scheme. For IS-95 systems,it is typically assumed that a minimum of 7 dB E_b/N_o is required for a voice call.

n Number of users in a cell.

α The voice activity factor, which is the fraction of time that the user is active in the channel. Self interference can be reduced by muting transmission during the pauses and a corresponding capacity gain can be achieved. α varies from 30-65% [23].

λ Sectorization Gain which is the gain achieved by reducing the total interference by sectorization of the cell. Usually, CDMA cells are divided into 3. $\lambda = 2.5$ is typical.

β Loading factor. This is defined as the ratio of other cell interference to same cell interference. In a single cell system it is 0, and can go up to 100% [10] as other cell interference increases. A typical value of β is 0.65 for outdoor cells.

F Frequency reuse factor given by $1/(1+\beta)$. The value is 1 for isolated cells and decreases as interference increases.

θ Orthogonality factor. As mentioned in Chapter 2, the forward link uses orthogonal codes for transmission which reduces the mutual interference between different users. The orthogonality factor is the ratio of the orthogonality that remains at the mobile after some of the orthogonality is reduced by multi-path propagation. The value is 1 for a perfect signal without multi-path and is nearly zero for a pure Rayleigh fading environment. Typically, it ranges from 0.4 to 0.7.

ρ Soft handoff gain, which is the forward link gain achieved by utilizing the maximal ratio combining of RAKE receivers. It can vary from 0.4 to 1.5 dB.

δ Soft handoff capacity overhead, which is the percentage increase in the number of channels that are used to support users in soft handoff. Usual system designs allow for 30% of the calls to be soft handoff, which results in a δ of 0.18.

P_{bts} The power transmitted by the base station for each user/channel, which is the sum of paging, sync and traffic channels. It is expressed in Watts or dBm.

χ Percentage of P_{bts} allocated to traffic channels of all users. Usually, it is 80%.

P_{mob} Power transmitted by the mobile. This varies from -55 dBm to 23 dBm.

NF_{bts} Noise figure of the base station, represented in dB.

NF_{mob} Noise figure of the mobile device, represented in dB.

NF_{das} Effective noise figure of the DAS unit, in dB.

U Total number of units in the DAS (Number of RAUs + Expansion Units + Main Hub Units).

η The background noise seen by the RAU antennas of the DAS which is $k \cdot T \cdot W$ where k is Boltzmann's constant and T is the absolute temperature. Usually represented in dBm.

ν The path loss exponent, which is the power of distance by which transmitted RF power is diminished. For free space, the path loss exponent is 2. The value of the path loss exponent varies from 1.8 to 6 depending on various environments [67].

L_0 Reference Path Loss. This is assumed to be 40 dB at a distance of 1 meter.

For CDMA communication systems, Frame Erasure Rate (FER) is a more important metric than BER because voice quality depends on FER. Bit errors can be corrected using Forward Error Correction codes (FEC) and a frame is in error only when the error correcting capability of FEC is exceeded [35]. The FER can be defined in terms of E_b/N_o and E_b/N_o can be defined in terms of S/N.

The energy per bit E_b is the product of average power per bit interval S and signal period T (inverse of bit rate R). E_b/N_o is given by (4.1):

$$\frac{E_b}{N_o} = \frac{ST}{N/W} = \frac{S}{N}\frac{W}{R} \tag{4.1}$$

The signal power S in the above expression is the power received P_r at the receiver after undergoing path loss (PL) due to large scale (log normal shadowing) and small scale fading (multi-path) and other losses such as cable loss. Several empirical and physical models exist to model the propagation losses encountered by the signal[12, 13, 14, 15]. For a typical DAS, the minimum path loss experienced by the signal in a line of sight environment close to the transmit antenna is around 40 dB. The path loss can be approximated using the single line slope model as (4.2) and in decibels as (4.3) where d is the distance from the transmitting antenna.

$$PL = L_0 \cdot d^{\nu} \tag{4.2}$$

$$\rightarrow PL(dB) = L_0(dB) + 10 \cdot \nu log(d) \tag{4.3}$$

We can express the reverse link received signal generally as (4.4) and forward link received signal as (4.5).

$$P_{R_{rvs}} = P_{mob} - PL(dB) \rightarrow P_{R_{rvs}}(dB) = P_{mob}(dB) - 10 \cdot log(L_0 \cdot d^{\nu}) \tag{4.4}$$

$$P_{R_{fwd}} = 10 \cdot log\left[\frac{\chi \cdot P_{bts_W}}{n(1+\delta)}\right] - PL(dB) \rightarrow P_{R_{fwd}}(dB) = 10 \cdot log\left[\frac{\chi \cdot P_{bts_W}}{n(1+\delta)}\right] - 10 \cdot log(L_0 \cdot d^{\nu}) \quad (4.5)$$

The noise N represents the sum of ambient thermal noise η, system generated noise, which is the sum of NF_{bts}, NF_{das} and NF_{mob}, and the interference I which is the sum of intra-cell interference (interference from users of the same cell) I_s and inter-cell interference (interference from neighboring cells) I_o. Even though it is very difficult to exactly model the interference as the users are distributed randomly in cells and suffer different propagation losses, several models exist in the literature to approximately calculate them. We can represent the total noise in the reverse link as (4.6) and the forward link as (4.7)

$$N_{rvs}(dBm) = NF_{bts}(dB) + NF_{das}(dB) + \eta \cdot W(dBm) \quad (4.6)$$

$$N_{fwd}(dBm) = NF_{mob}(dB) + NF_{das}(dB) + \eta \cdot W(dBm) \quad (4.7)$$

Under perfect power control, the received power from every mobile in a cell will be the same. Hence using loading factor and voice activity factor and the sectorization gain, we can represent the total reverse link interference in Watts as (4.8):

$$I_{rvs} = I_s + I_o = I_s + \beta.I_s = \quad (n-1)P_{R_{rvs}} + \beta(n-1)P_{R_{rvs}} = \quad (1+\beta)(n-1)\big(\frac{\alpha}{\lambda}\big)P_{R_{rvs}} \quad (4.8)$$

In the forward link, the interference is scaled by the orthogonality factor θ and soft handoff gain ρ while the number of users is scaled up by the soft handoff overhead δ. Thus total forward link interference in Watts can be represented as (4.9)

$$I_{fwd} = (1+\beta)(1-\theta)(n(1+\delta)-1)\big(\frac{\alpha}{\lambda}\big)P_{R_{fwd}} \quad (4.9)$$

Substituting the above expressions in equation (4.1), we can express the $\frac{E_b}{N_o}$ in Watts for the reverse link as:

$$\frac{E_b}{N_o} = \frac{W}{R}\frac{P_{R_{rvs}}}{(NF_{bts} \cdot NF_{das} \cdot \eta \cdot W) + (1+\beta)(n-1)\big(\frac{\alpha}{\lambda}\big)P_{R_{rvs}}} \quad (4.10)$$

which gives us the received power in the reverse link as:

$$\rightarrow P_{R_{rvs}} = \frac{\big(\frac{E_b}{N_o}\big) \cdot NF_{bts} \cdot NF_{das} \cdot \eta \cdot W}{\frac{W}{R} - \big(\frac{E_b}{N_o}\big)\big(1+\beta\big)(n-1)\big(\frac{\alpha}{\lambda}\big)} \quad (4.11)$$

Finally, considering the reduction in the transmitted power for DAS in the reverse link as given in equation (3.4), the transmitted power by the mobile in dB can be written as (4.12):

$$\begin{aligned} \rightarrow P_{mob}(dB) &= 10 \cdot log(L_0 \cdot d^{\nu} \cdot U^{-\frac{\nu}{2}}) + 10log\left[\frac{\left(\frac{E_b}{N_o}\right) \cdot NF_{bts} \cdot NF_{das} \cdot \eta \cdot W}{\frac{W}{R} - \left(\frac{E_b}{N_o}\right)(1+\beta)(n-1)\left(\frac{\alpha}{\lambda}\right)}\right] \\ &= 10 \cdot log\left[\frac{\left(\frac{E_b}{N_o}\right) \cdot NF_{bts} \cdot NF_{das} \cdot \eta \cdot W \cdot L_0 \cdot d^{\nu} \cdot U^{-\frac{\nu}{2}}}{\frac{W}{R} - \left(\frac{E_b}{N_o}\right)(1+\beta)(n-1)\left(\frac{\alpha}{\lambda}\right)}\right] \end{aligned} \tag{4.12}$$

Similarly for the forward link, $\frac{E_b}{N_o}$ is given by:

$$\frac{E_b}{N_o} = \frac{W}{R}\frac{P_{R_{fwd}}}{(NF_{das} \cdot NF_{mob} \cdot \eta \cdot W) + (1+\beta)(1-\theta)(n(1+\delta)-1)\left(\frac{\alpha}{\lambda}\right)P_{R_{fwd}}} \tag{4.13}$$

After some rearrangement, we get the received power of the traffic channel in the forward link as:

$$\rightarrow P_{R_{fwd}} = \frac{\left(\frac{E_b}{N_o}\right) \cdot NF_{das} \cdot NF_{mob} \cdot \eta \cdot W}{\frac{W}{R} - \left(\frac{E_b}{N_o}\right)(1+\beta)(1-\theta)(n(1+\delta)-1)\left(\frac{\alpha}{\lambda}\right)} \tag{4.14}$$

In addition,the mobiles receive a constant power from the forward link pilot and access channels. Finally, considering the soft handoff gain and reduction factor from equation (3.3), we can express the transmitted power of the traffic channel by the BTS in dB as (4.15):

$$\begin{aligned} \rightarrow P_{bts}(dB) &= 10 \cdot log(L_0 \cdot d^{\nu} \cdot U^{1-\frac{\nu}{2}}) - 10.log\left[\frac{\chi}{n(1+\delta)}\right] \\ &+ 10log\left[\frac{\left(\frac{E_b}{N_o}\right) \cdot NF_{das} \cdot NF_{mob} \cdot \eta \cdot W}{\frac{W}{R} - \left(\frac{E_b}{N_o}\right)(1+\beta)(1-\theta)(n(1+\delta)-1)\left(\frac{\alpha}{\lambda}\right)}\right] - \rho(dB) \\ &= 10log\left[\frac{L_0 \cdot d^{\nu} \cdot U^{1-\frac{\nu}{2}} \cdot \left(\frac{E_b}{N_o}\right) \cdot NF_{das} \cdot NF_{mob} \cdot \eta \cdot W\left(\frac{n(1+\delta)}{\chi}\right)}{\frac{W}{R} - \left(\frac{E_b}{N_o}\right)(1+\beta)(1-\theta)\left[n(1+\delta)-1\right]\left(\frac{\alpha}{\lambda}\right)}\right] - \rho(dB) \end{aligned} \tag{4.15}$$

We plot the above equations for various values of n and U in the following section.

4.2 Operating Region of a DAS

We assume the following values for the discussion below:

Bandwidth of the channel W	: 1.2288 MHz
Data rate R	: 9.6 kbps
$\frac{E_b}{N_o}$	: 7 dB
Voice activity factor α	: 0.32
Loading factor β	: 0.65
Sectorization gain λ	: 1 (We consider 1 sector only)
Background noise η	: -174 dBm/Hz
Orthogonality factor θ	: 0.7
Soft handoff gain ρ	: 0.4
Soft handoff capacity overhead δ	: 0.18
Percentage power for traffic channels χ	: 0.8
Base station noise figure NF_{bts}	: 5 dB.
Mobile noise figure NF_{mob}	: 8 dB.
DAS gain	: 0 dB.
DAS noise figure NF_{das}	: 25 dB.
Number of DAS units U	: 100 (RAUs+Expansion Hubs+Main Hubs)
Mobile forward link minimum power	: -117 dBm [1] .
Mobile forward link maximum power	: -25 dBm.[68].
Mobile reverse link minimum power	: -55 dBm [69].
Mobile reverse link maximum power	: 23 dBm.
BTS forward link minimum power	: -108 dBm.
BTS forward link maximum power	: 43 dBm (20 W) [70].
BTS reverse link minimum power	: -105 dBm
BTS reverse link maximum power	: -75 dBm.

4.2.1 Numerical results

It can be seen from the figures below that a CDMA DAS system is always reverse link limited. Figure 4.1 shows the received power at the mobile on the forward link for various number of users. Figure 4.2 shows the corresponding transmit power from the base station, assuming a distance of 25 meters from the antenna. For both forward and reverse directions, DAS system is assumed to have 100 RAUs and a noise figure of 25 dB.

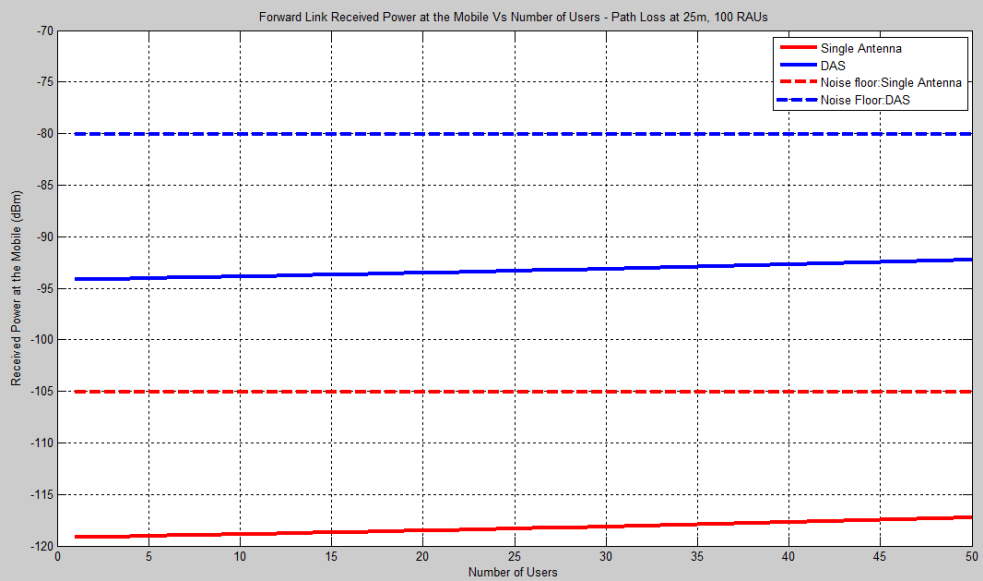

Figure 4.1: Plot showing forward link received power at the mobiles Vs the number of users, DAS noise figure = 25 dB

It may be observed that, the noise floor in the DAS scenario is higher than the single antenna scenario by 25 dB. The relative increase in received power level is very small, as the number of users go up. Even though the base station has to transmit at higher power in the DAS scenario, it is well below the maximum power level (43 dBm assumed).

Figures 4.3 and 4.4 shows the reverse link received power at the base station and transmitted power of the mobiles respectively, both with respect to the number of users. The users are assumed to be at an average distance of 25 meters from the nearest antenna.

We can see from the figures that the reverse link runs out of capacity, much quicker than the

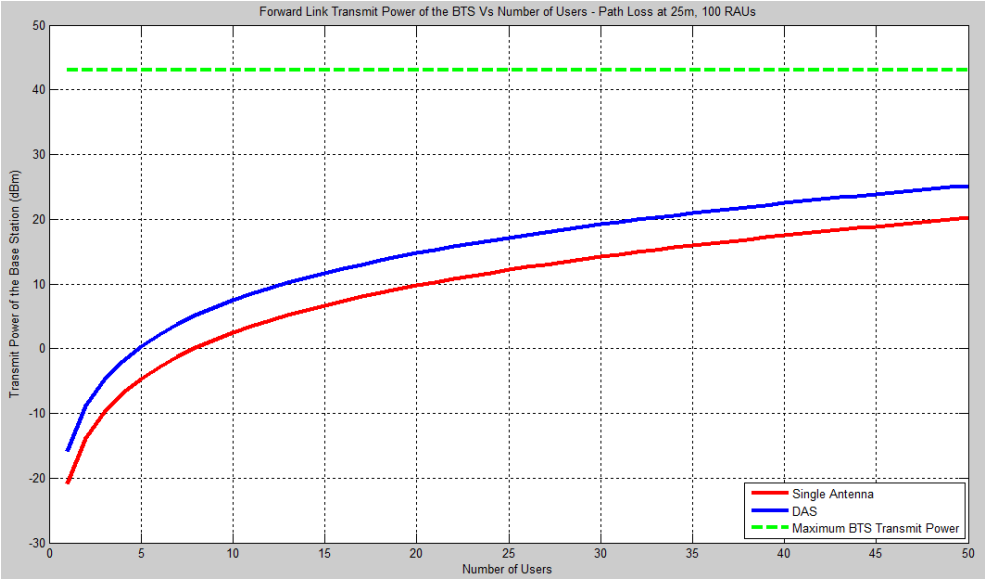

Figure 4.2: Plot showing forward link transmitted power of the base station Vs number of Users , DAS noise figure = 25 dB

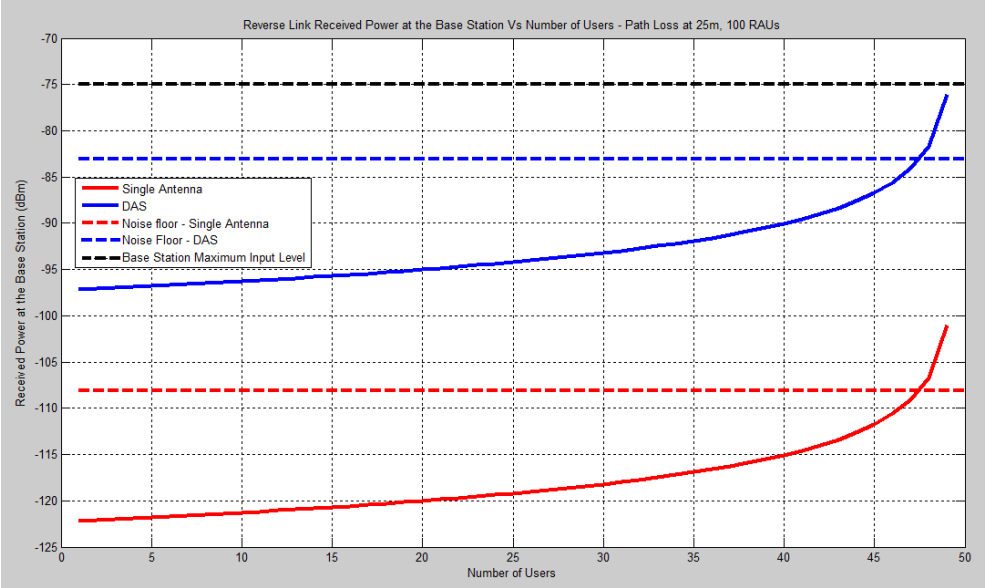

Figure 4.3: Plot showing reverse link received power at the base station Vs number of users; DAS Noise Figure = 25 dB

forward link. Hence, we can conclude that DAS systems are capacity limited on the reverse link.

It is interesting to see that for the same received power at the base station, mobiles have to transmit less power in the DAS scenario. This is due to the fact that they suffer less path loss. This

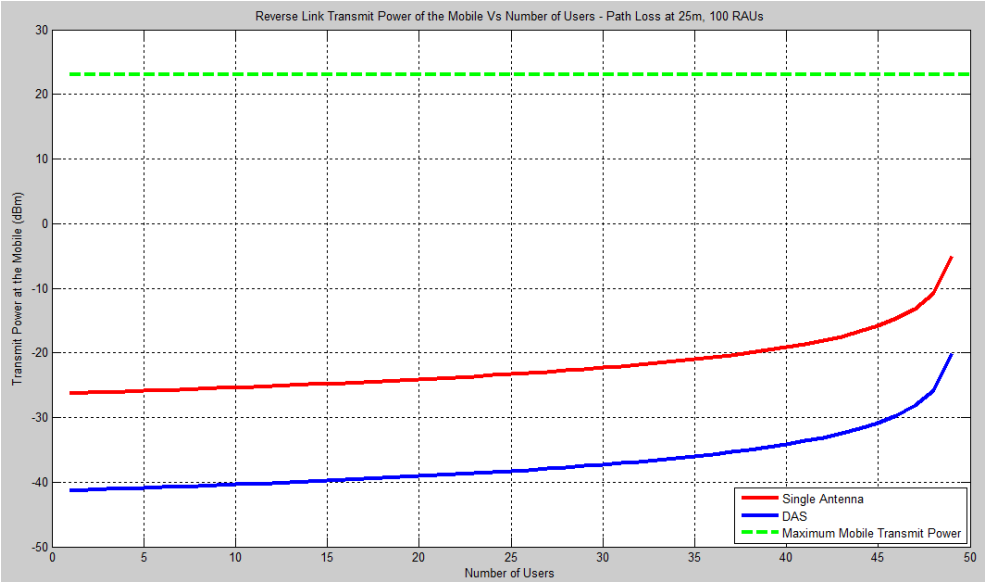

Figure 4.4: Plot showing reverse link transmit power of the mobile; DAS Noise Figure = 25 dB, Average Distance = 25 m

observation supports the theoretical results showing increased capacity of DAS systems. However, we can see that the higher noise floor at the base station limits the capacity as the received power level rises beyond the base station dynamic range (-75 dBm assumed here), even if the mobiles transmit well below their maximum power. The system is said to be noise limited in this situation.

It can also be seen that as path loss increases, the transmit power of the mobiles also increases until it reaches the maximum transmit power (+23 dBm). The system is said to be coverage limited in this situation.

It may be noted from the equation (4.12), that the transmitted power of the mobile depends on noise figure of the DAS (NF_{das}), the path loss (d^{ν}) and power reduction which is a function of the path loss exponent ($U^{-\frac{\nu}{2}}$). The Figure 4.4 indicates this difference (for a constant path loss, $25(NF_{das} - 40$(Power gain) $= -15$ dB). Generally, there will be a net reduction in transmit power for any value of path loss greater than 2. Figure 4.5 shows the relative values of DAS noise figure and the transmit power gain for values path loss exponents.

Figure 4.6 shows the mobile transmit power for various number of RAUs. It can be seen that as DAS grows in size, it has lesser impact on the mobile transmit power. Finally, figure 4.7 shows

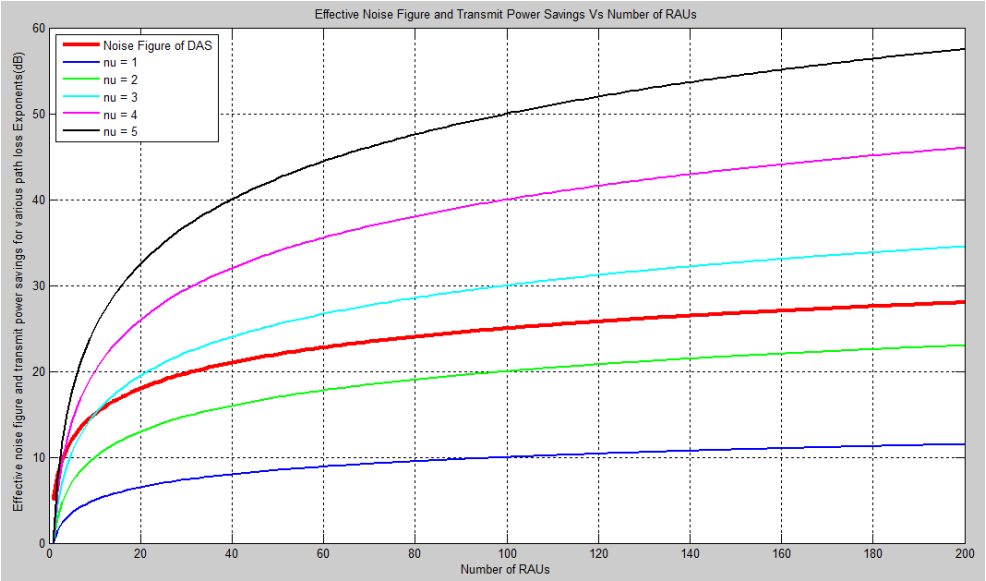

Figure 4.5: Plot comparing DAS noise figure with power savings factor for various path loss exponents

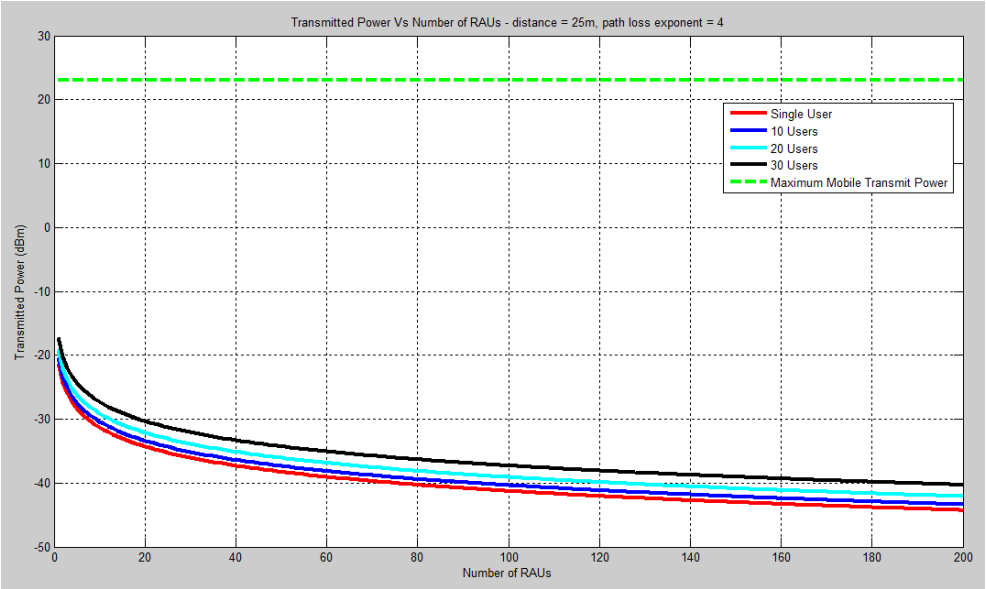

Figure 4.6: Plot showing reverse link transmit power Vs number of RAUs, path loss exponent = 4

the mobile transmit power versus distance, for single antenna system and the DAS system. The graph is plotted for a single user, at a distance of 25 m from the antenna. It is clear that because of the reduction in transmit power, DAS can provide coverage to a larger area, compared to the single antenna system.

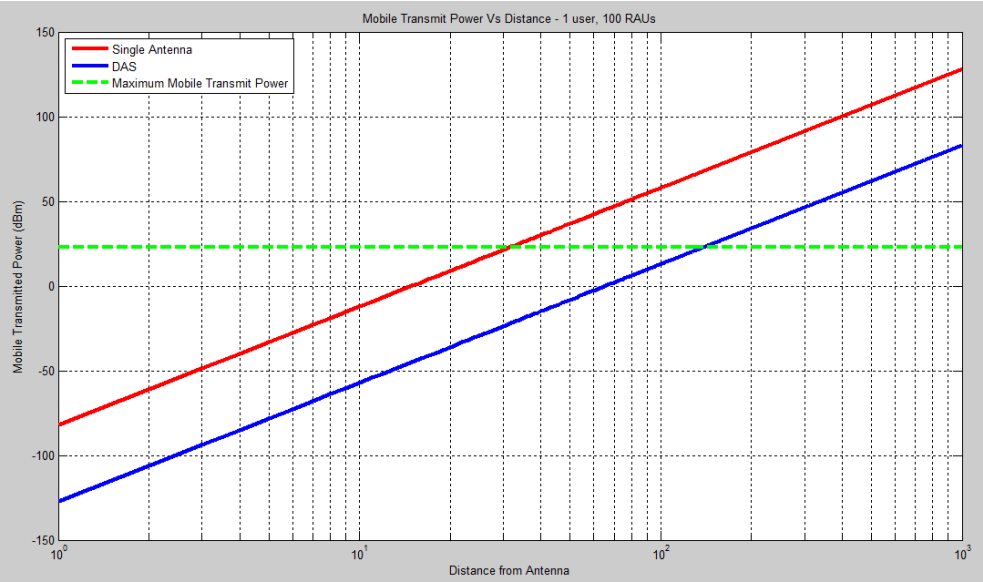

Figure 4.7: Plot showing reverse link transmit power Vs distance, path loss exponent = 4, single user case

Chapter 5

Measurements: Setup and Data

Several sets of measurements were conducted on a large and complex DAS system to understand its performance and identify the situations in which DAS displays unexpected behavior.

The DAS system on which measurements are conducted is an Active Hybrid Fiber Coax system that is fed by two base stations and caters 11 buildings in a large corporate campus, with approximately 16,000 users. It is deployed using ADC/Tyco InterReach family of products namely InterReach Spectrum, InterReach Fusion and InterReach Unison.

In this chapter, architectural details of the DAS system on which measurements were made, specifications of various active and passive components that make up the DAS and the details of various measurement set up are described. Measured data and various observations are also detailed.

5.1 System Overview

Two Nortel Base Stations, one for cellular (850 MHz) and the other for PCS (1900 MHz), feed the DAS system dividing the entire area into three sectors. The entire DAS system consists of 34 Unison Main Hubs (17 for each band), 5 Fusion Main Hubs, 104 Unison Expansion Hubs (52 for each band), 14 Fusion Expansion Hubs, 650 Unison Remote Antenna Units (RAUs - 325 for each band) and 97 Fusion RAUs. These units are connected to the base stations using 4 Spectrum Host Units, 11 Dart Remote Units (DRUs) and 11 Main Remote Access Units (MRAUs). The Host Units and DRUs are interconnected using three Fiber Rings that run across the whole campus.

For the purpose of measurements, we focused on a single sector in the cellular band. This sector serves a single building with approximately 8000 users. The building is served by 6 channels belonging to the cellular A band (ranging from 825.03 MHz to 834.33 MHz). Each channel is 1.2288 MHz wide. The center frequencies of these channels are given in Table 5.1.

Table 5.1: Cellular Channels of Sector 1 and their Frequencies

Channel Name	Channel Number	RL Frequency (MHz)	FL Frequency (MHz)	Service
F1	283	833.49	878.49	1x Voice
F2	242	832.26	877.26	1x Voice
F3	201	831.03	876.03	1x Voice
F4	160	829.8	874.8	1x Voice
F5	119	828.57	873.57	1x Voice
F7	37	826.11	871.11	EV-DO Data

The schematic diagram illustrating this portion of the DAS is shown in Figure 5.1. It consists of 3 Main Hubs, 10 Expansion Hubs and 66 RAUs spread across the building. The DAS is built using the ADC InterReach Spectrum product at the head-end and the InterReach Unison product at the far-end. The Unison equipment is connected in a star configuration. Table 5.2 shows the various elements of the DAS and parameters that characterize them.

Even though there are losses involved with connectors and cabling, the ADC InterReach Unison system is designed in such a way that the losses are compensated for. Hence using equation 3.25 with all gain factors = 1 and the values from Table 5.1, we can calculate the effective noise figure and the gain of the entire system as:

$$\begin{aligned} \text{Reverse link noise figure up to the MRAU} &= 3 \cdot NF_{MH} + 10 \cdot NF_{EH} + 66 \cdot NF_{RAU} \\ &= 10 \cdot log(10 \cdot 6.91 + 66 \cdot 3.09) \\ &= 24.36 \quad dB \end{aligned} \tag{5.1}$$

$$\begin{aligned} \text{Reverse link gain up to the MRAU} &= -10 \cdot log(\text{Number of Main Hubs}) \\ &= -10 \cdot log(3) \\ &= -4.7 \quad dB \end{aligned} \tag{5.2}$$

We can see that the rest of the system is cascaded up to the base station, with noise figures contributed by the MRAU, DRU and the Fiber Ring. Using Friis' Cascaded Noise Figure equation (5.3), we can write the reverse link noise figure up to the Spectrum Host as (5.4):

$$F = F_1 + \frac{F_2 - 1}{G_1} + \frac{F_3 - 1}{G_1.G_2} + \cdots + \frac{F_n - 1}{G_1.G_2 \cdots G_{n-1}} \tag{5.3}$$

Reverse link noise figure up to the Spectrum Host

$$= 10 \cdot log\left[10^{24.36/10} + \frac{10^{6.9/10} - 1}{10^{-4.7/10}} + \frac{10^{10.4/10} - 1}{10^{-4.7/10}} + \frac{10^{8/10} - 1}{10^{-4.7/10}}\right] = 25.17 \quad dB \tag{5.4}$$

Assuming the room temperature to be 290K, we can calculate the expected noise floor at the Spectrum Host as:

$$\text{noise floor} = k.T_0 + \text{noise figure} = -174 + 25.17 = -148.8 \quad dBm/Hz. \tag{5.5}$$

For the CDMA channel of 1.2288 MHz, the expected noise floor is thus -87.9 dBm/channel.

5.2 Measurement Setup

Measurements were obtained from 3 different locations in the DAS network for a continuous period of time. These measurement methods and the data obtained are described below.

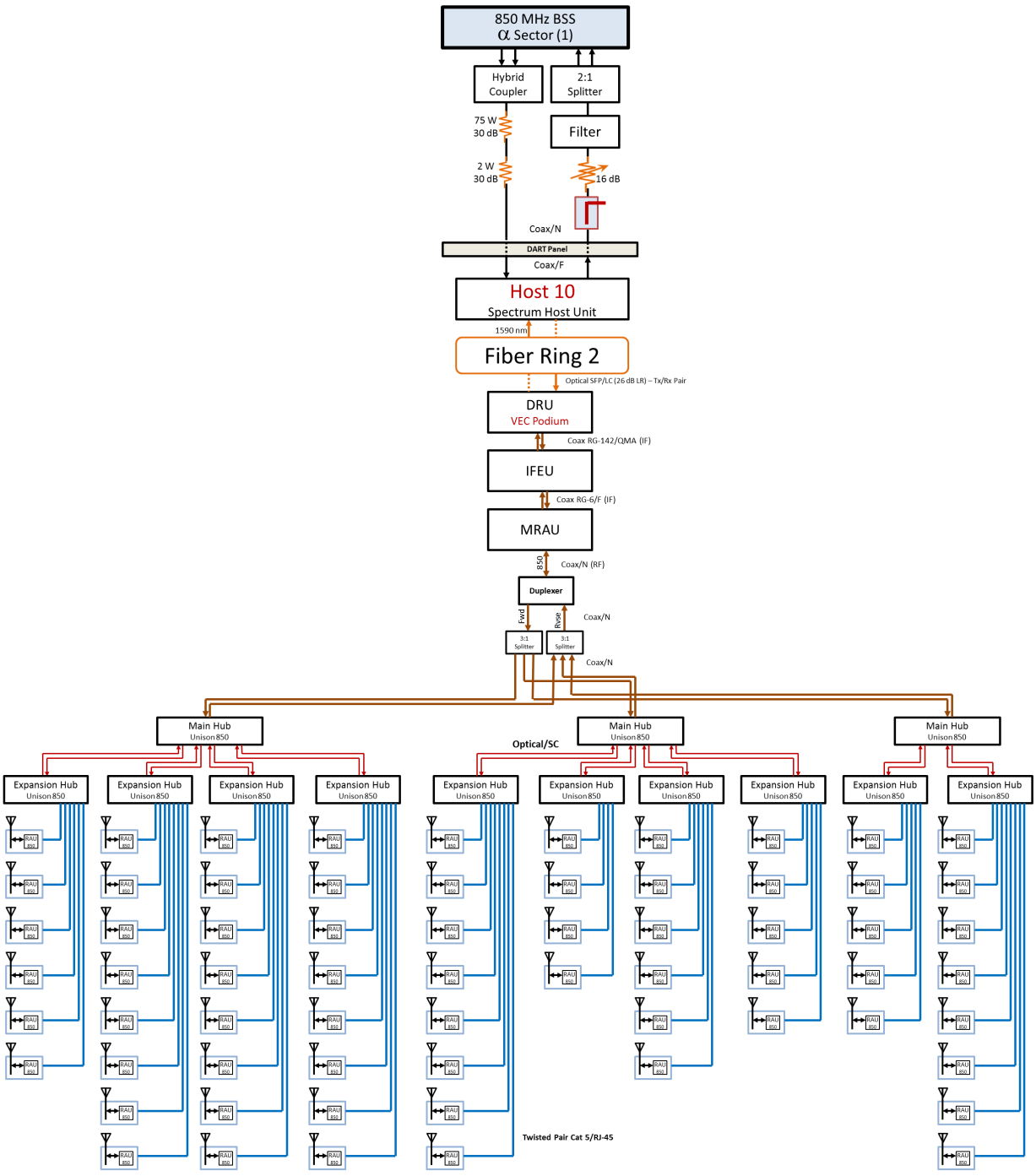

Figure 5.1: Schematic of the DAS which serves sector 1, operating in the cellular band (850 MHz).

Table 5.2: DAS components and their Characteristic Values

Item	Noise Figure (dB)	Gain/Loss (dB)	Connector Loss (dB)
Antenna		4 dBi	
2 Ft Coax/SMA Cable		-0.2	-0.06
RAU	4.9		
Cat 5e/RJ45 Cable		-24	-2.2
Expansion Hub	8.4		
Optical/SC Fiber		-0.03	-0.4
Main Hub	0		
Coax/N Cable		-20	-0.3
Splitter/Combiner		-5.27	-1.0
Coax/N Cable		-2	-0.3
Duplexer		-40	-1.5
Coax/N Cable		-2	-0.3
MRAU	6.9		
Coax RG6/F Cable		-0.25	-0.3
IFEU	0		
Coax RG142/QMA Cable		-1	-0.3
DRU	10.4		
Optical/SC(SFP)Cable		-3	-1
Fiber Ring	8		
Optical/SC(SFP)Cable		-3	-1
Spectrum Host	0		
Coax/F Cable		-0.25	-0.3
Measurement Coupler		-0.1	
Coax/N Cable		-1	-0.3
Variable Attenuator		-16	
Coax/N Cable		-1	-0.3
RF Systems Filter		-1.9	
Coax/N Cable		-1	-0.3
Hybrid Coupler/Splitter		-0.5	
Coax/N Cable		-1	-0.3
Base Station	2		

5.2.1 Switch Data

Network traffic information available from the switch was collected continuously for a period of 24 hours. The data contain detailed call information for all calls served on sector 1, on November 8th, 2011 from 12.00 AM to 11.59 PM. The Figure 5.2 shows the numbers of active calls at the start of every minute on individual channels as well as total number of calls on all channels. It can be observed that the traffic is at peak rates around 9:30 AM and 2:30 PM. The channels are loaded approximately at the same rate.

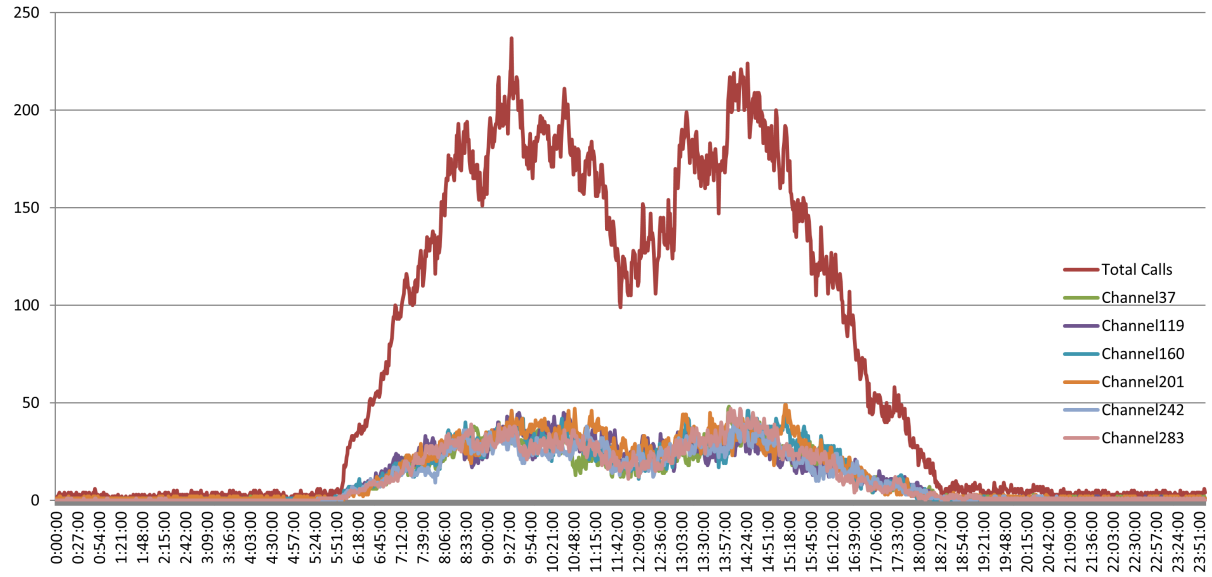

Figure 5.2: Graph showing the number of calls at the start of every minute for a period of 24 hours

5.2.2 Spectrum Analyzer Data

A spectrum analyzer was attached to the directional coupler depicted in Figure 5.1. A low noise amplifier (LNA) was connected at the input of the Spectrum Analyzer so that weak signals could also be captured in the measurements. The exact measurement setup is shown in Figure 5.3. A spectrum trace across the cellular band was captured every 60 seconds using a script that communicates with the spectrum analyzer from a computer via the VX-11 Protocol. Various parameters used for the spectrum analyzer measurements are given in Table 5.3.

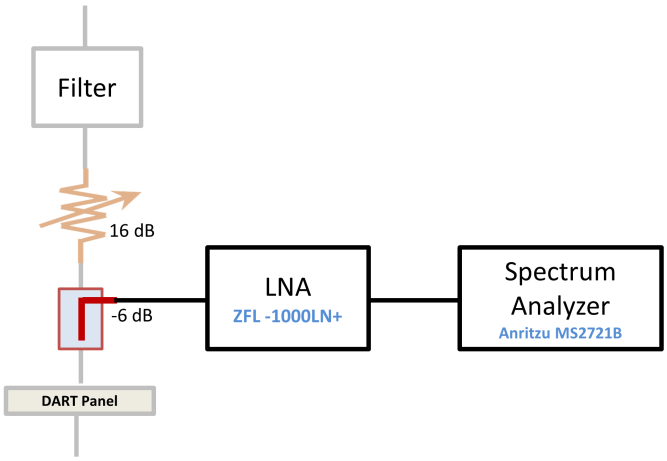

Figure 5.3: Schematic of spectrum analyzer connected to the directional coupler and low noise amplifier

Table 5.3: Spectrum Analyzer Measurement Parameters

Parameter	Value
LNA Noise Figure	3 dB [71]
LNA Gain	23.5 dB (for 15V) [71]
Spectrum Analyzer Frequency Span	824 MHz - 850 MHz
Resolution Bandwidth (RBW)	30 KHz
Video Bandwidth (VBW)	10 KHz
Reference Level	-65 dBm
Reference Level Offset	0 dB
Input Attenuation	0.0 dB
Preamp	ON
Scale	5 dB/div
Trace Mode	Average
Trace Count	50
Markers	1 (825.03 MHz), 2 (835 MHz) and 3 (846.36 MHz)

Assuming a standard thermal noise of -174 dBm/Hz, total connector and cable losses of 2.5 dB and total noise contribution by the coupler and connectors of 6 dB, we can express the total input noise to the Spectrum Analyzer as:

$$\begin{aligned} \text{Input noise to Spectrum Analyzer} &= -174 + 25.17 - 6 + 23.5 + 3 - 2.5 + 6 \\ &= -124.83 \quad dBm/Hz. \end{aligned}$$

At no input to the Spectrum Analyzer, the Displayed Average Noise Level (DANL) when the

preamp is ON is -163 dBm/Hz. Also, the total noise floor will go down by 24 dB when preamp is ON as the Spectrum Analyzer keeps the maximum level same, irrespective of preamp status [72]. Hence, the effective noise floor level displayed in the Spectrum Analyzer traces, for a resolution bandwidth of 30 KHz is:

$$\begin{aligned} \text{Effective noise floor displayed} &= 10 \cdot log\left(10^{-124.83/10} + 10^{-163/10}\right) + 10 \cdot log(30,000) - 24 \\ &= -104.05 \quad dBm. \end{aligned}$$

Figures 5.4 and 5.5 are the examples of plots obtained at 2:30 PM and 9:30 AM respectively. Markers 1 and 2 indicate the beginning and end of Cellular A band (825.03 MHz and 834.33 MHz). CDMA activity in the A band and the W-CDMA signal from the neighboring B band can be clearly observed. The noise floor level of -104.05 dBm is also visible from the figures.

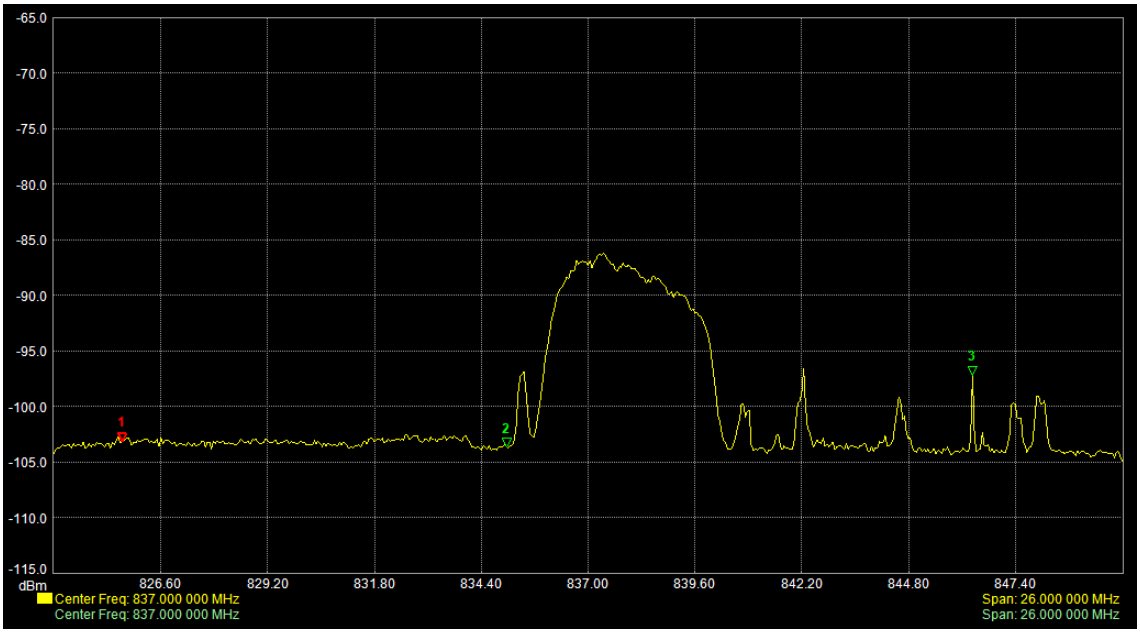

Figure 5.4: Example plot obtained using Spectrum Analyzer at 2:30 PM on October 24th, 2011

5.2.3 Continuous wave test signal

To observe the gain changes of the DAS that result from increased traffic, a continuous wave signal was set up using a Praxsym Personal Test Transmitter in an unused channel (846.36 MHz,

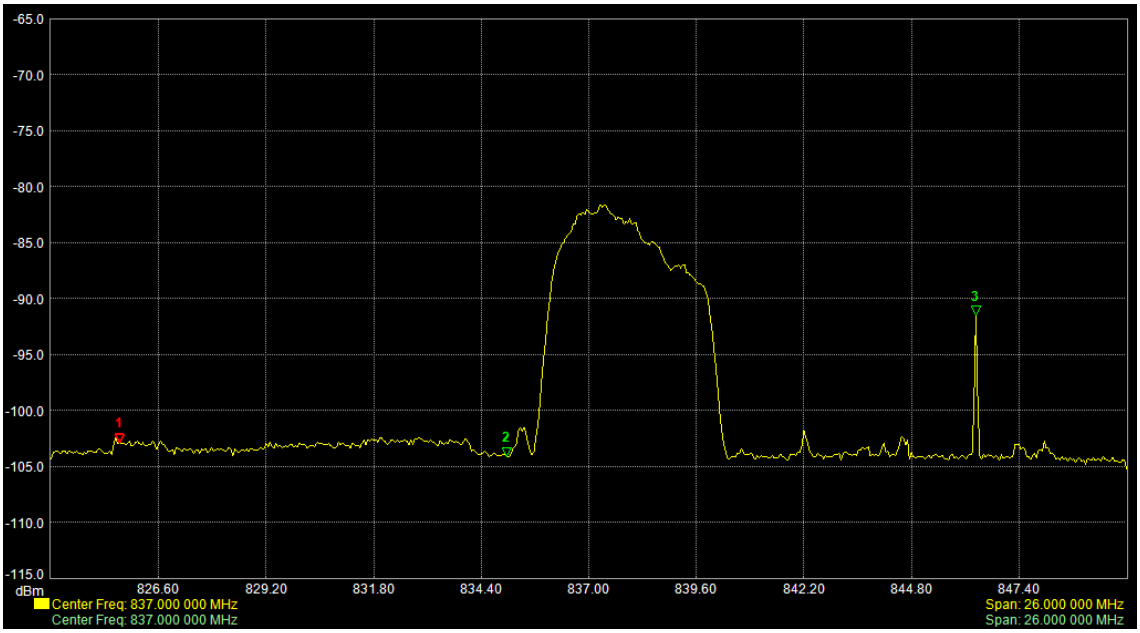

Figure 5.5: Example plot obtained using Spectrum Analyzer at 9:30 AM on October 25th, 2011

indicated by marker 3) so that variations in the received power of this signal with respect to traffic activity could be observed. The signal source transmits at -10 dBm, located 30 feet away from an RAU. Figure 5.6 shows the variation of received power of this test signal from 12:00 PM on October 24th, 2011 to 11:59 AM on October 25th, 2011. As can be observed, no correlation is seen between the traffic and the test signal pattern. The received strength remained constant during the night, and varied only during office hours, indicating that movement of people has a considerable effect on the received signal strength.

5.2.4 Reported Power from DRU

The Dart Remote Unit (DRU) is enabled with the ability to report the maximum, average and minimum power level in the full cellular band (824 MHz - 849 MHz). This information is captured every 60 seconds for a period of 24 hours using a script that communicates with the DRU over IP using SNMP protocol. Continuous measurements were made for the periods 10:30 AM to 4:00 PM (Oct 24th), 7:00 PM (Oct 24th) to 1:00 AM (Oct 25th) and 7:30 AM to 1:00 PM (Oct 25th), each representing different diurnal activity levels. Figures 5.7, 5.8 and 5.9 show the measurements.

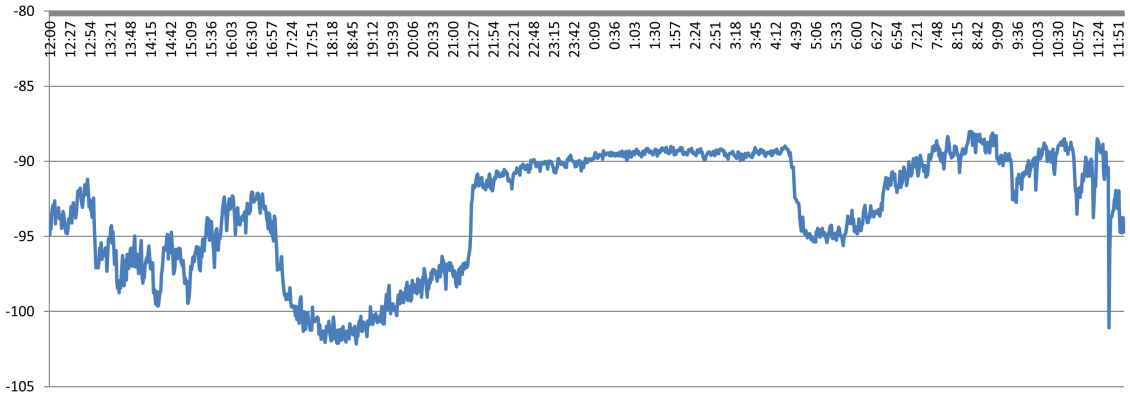

Figure 5.6: Plot showing the received strength of the test signal at 846.36 MHz for a duration of 24 hours.

Comparing the figures, it can be observed that the received power level increases when traffic activity is higher. For example, in Figure 5.7, the traffic activity is higher and corresponding maximum power level is around -55 dBm, while in Figure 5.8, the traffic activity is lower and corresponding maximum power level is around -70 dBm.

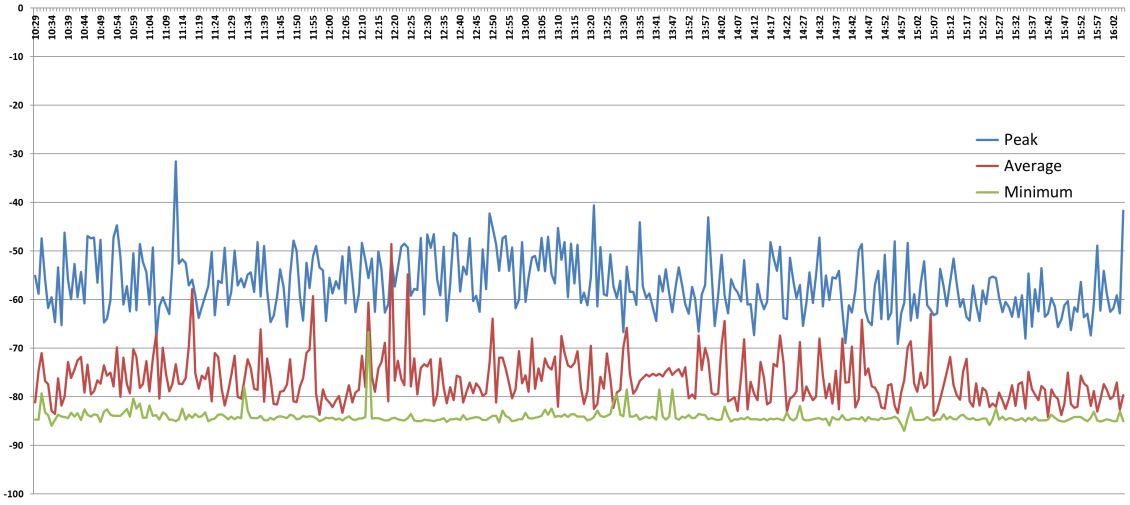

Figure 5.7: Plot showing the received signal power at the DRU from 10:30 AM to 4:00 PM on October 24th

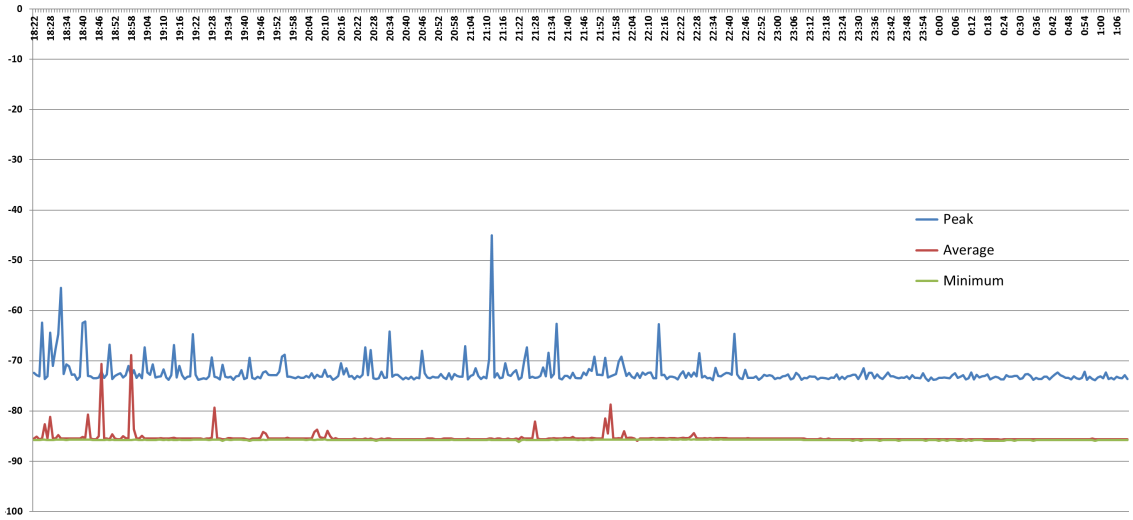

Figure 5.8: Plot showing the received signal power at the DRU from 7:00 PM (Oct 24) to 1:00 AM (Oct 25)

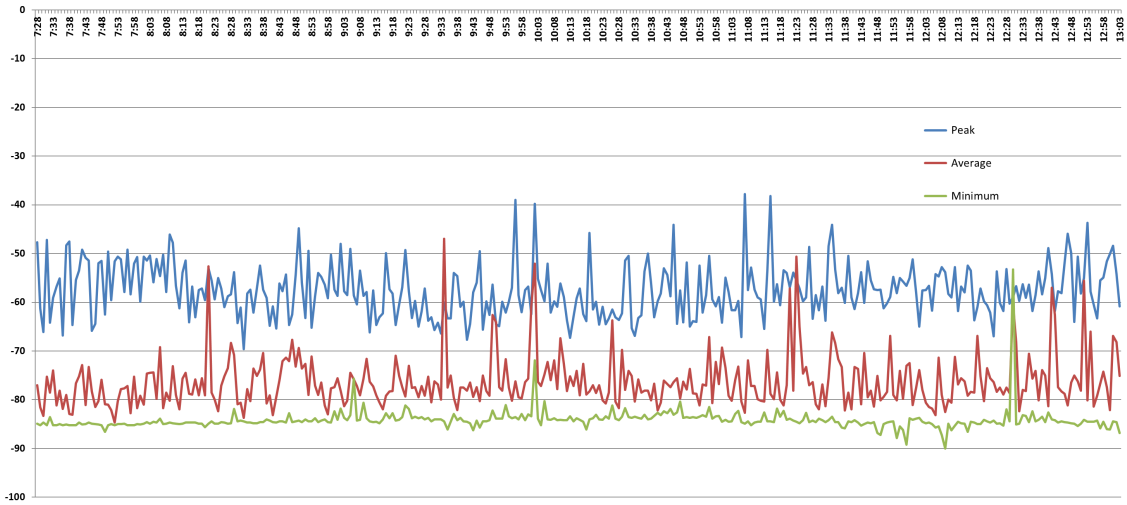

Figure 5.9: Plot showing the received signal power at the DRU from 7:30 AM to 1:00 PM on October 25th

Chapter 6

Important Observations

We made 3 important observations during the measurement process, which appear to reduce the reverse link capacity. Due to lack of sufficient data, we were unable to completely validate the theoretical model of DAS, described in chapter 4.

6.1 Reverse Link Padding

DAS systems have a significant noise figure, which raises the noise floor seen by the base station on the reverse link. This results in higher power levels at the base station, thereby driving it into a non-linear operating region. Network operators have alarms in place to notify of high input reverse link power. In order to bring down the noise floor and prevent alarms, a common practice is to use attenuator padding at the DAS front end so that the noise floor is brought down. This set up is shown in Figure 6.1.

Even though inserting the pad can eliminate the effect of DAS on the noise floor, it has an opposite effect on the transmitted signal level of the mobile. As we can see from figure 6.2, the mobiles see a higher noise barrier looking towards the base station and will be required to transmit a power equal to the sum of DAS noise figure and attenuator noise figure in addition to the power it would have transmitted in a single antenna case. This will reduce the reverse link capacity of the system as mobiles run out of transmit power quickly, with an increased number of users.

Figure 6.3 shows the transmitted power of mobiles in the presence of DAS. Comparing with Figure 4.4, we see that mobiles transmit at higher power in the DAS case.

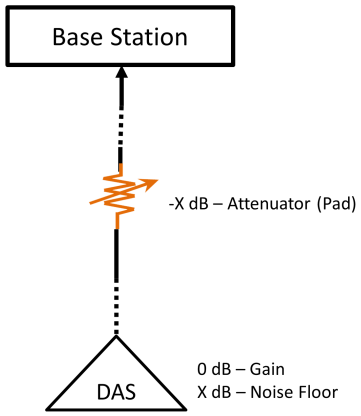

Figure 6.1: Pad inserted in front of the BTS to reduce the increased input power by the DAS

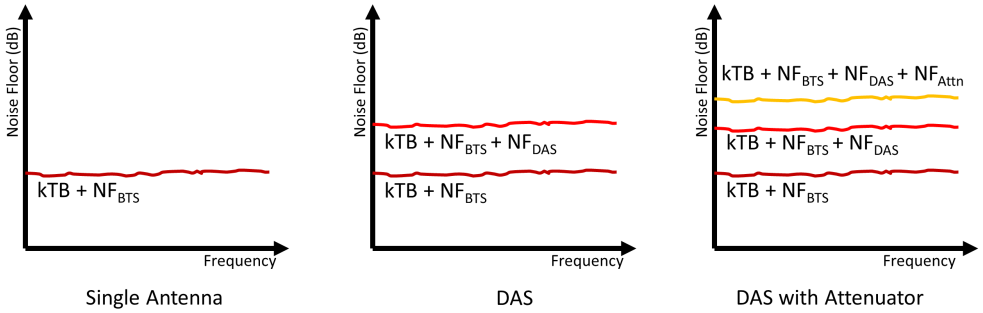

Figure 6.2: Mobiles have to overcome a higher noise barrier by transmitting at higher power levels

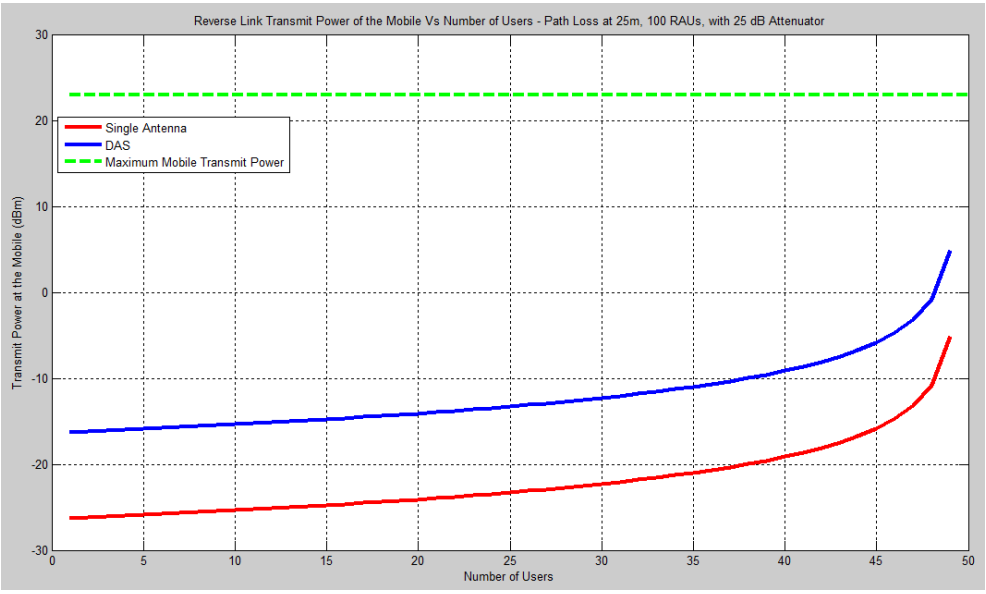

Figure 6.3: Mobiles transmit at higher power levels due to the presence of attenuator pad

6.2 BART Spikes

In a CDMA system, the reverse link power of all carriers is expected to be equal. This is achieved by power control so that the received power from all mobiles will be equal at the base station.

During the measurement process, it is observed that the expected balance between carriers is broken at times. For a short duration ranging from a few seconds to 3 minutes, the power received at a given carrier frequency would be higher relative to other carriers in the system. Examples of this phenomenon are shown in figures 6.4 and 6.5.

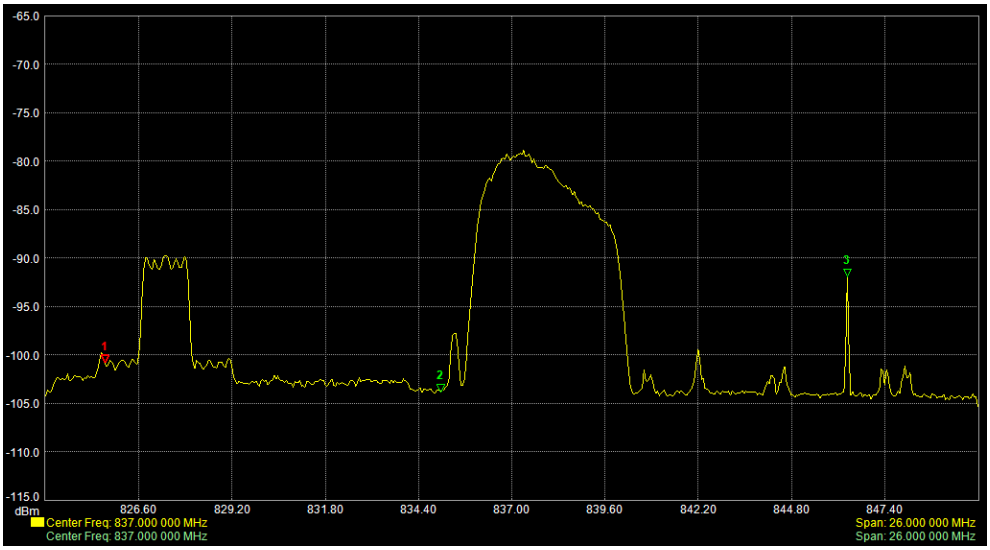

Figure 6.4: Different carriers in the same sector have relatively different transmit power levels, resulting in BART spikes

These spikes appear to be randomly occurring for short periods of time and were observed to occur randomly at all carrier frequencies. We named these phenomena 'BART spikes'. Identifying the root cause of these spikes is beyond the scope of this thesis. However it may be because of one or more of the following reasons.

(1) One or more mobiles operating on the specific carrier frequency gets too close to the antenna and cannot turn down the power anymore. This means more power is transmitted than required, which results in a need for other mobiles transmitting on the same carrier

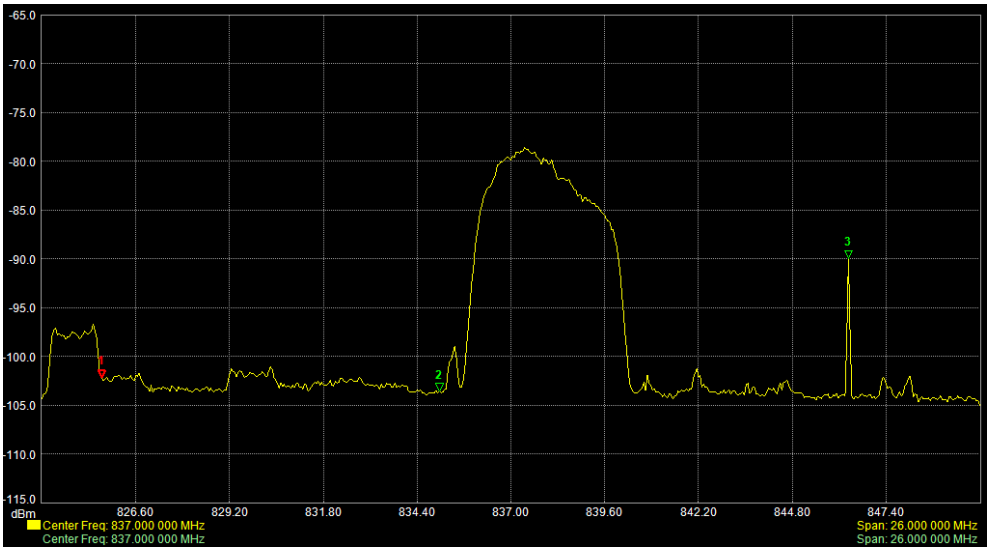

Figure 6.5: Different carriers in the same sector have relatively different transmit power levels: another example of BART spikes

frequency to increase their levels, so as to be at the same power level at the receiver.

(2) A mobile physically present in the DAS coverage region tries to communicate to an outside cell. This could happen if an overlap region exists between the DAS and outside cell.

(3) An external source, which is unrelated to the cellular system, causes in-band interference resulting in mobiles raising their transmit power.

6.3 Out-of-Band Noise

The antennas and the ADC Unison RAUs are designed to operate across the entire cellular band. As a result, out-of-band signals are also received by the RAUs, which are transferred through the DAS, until they are filtered out by filters just before the BTS. A W-CDMA signal in the B band is clearly visible in figures 6.4 and 6.5. These out-of-band signals are strong since they are transmitted by mobiles attempting to communicate to a BTS that is outdoors and far away.

Even though out-of-band signals do not have an effect at the base station as they are filtered out, they will increase the average power received at the RAUs. This results in the risk of activating the Automatic Level Controls (ALC) at the RAUs. If ALCs are not set at a sufficiently high

threshold, they will try to reduce the overall power level, which in turn will have a negative effect on the CDMA signals also. We suggest three solutions to this issue:

(1) For the case of single band DAS operation, specially designed antennas suitable to be operated in the band of interest should be used. This could prove to be an economical solution to this common cross-band input to single user DAS.

(2) Automatic level control in the RAUs should be designed in such a way that they are configurable for a particular band. This will help eliminate the unwanted signals and corresponding energy that may otherwise be carried through the DAS.

(3) Filtering on the RAUs for specific band would be the best solution. However, this is not an economically desirable solution as it requires non-uniform hardware development.

.

Chapter 7

Conclusion

The importance of DAS systems in indoor wireless networks is significant. DAS systems are becoming increasingly important in modern cellular systems as they carry traffic to the buildings and provide better RF performance. DAS are becoming larger and more complex. This fact necessitates the proper standardization of DAS design and signifies the requirement of strong theoretical results pertaining to the performance of DAS systems. In this thesis, we have outlined the practical limitations of CDMA based DAS systems and introduced a mathematical framework which can be used in DAS design.

We laid out the operating region of a CDMA based DAS system for various parameters such as number of users and number of RAUs, and discussed its performance under various situations. Following are the important conclusions from this work.

7.1 Two Observations

(1) Distributed Antenna Systems provide considerable higher capacity and coverage, compared to traditional single antenna systems. However there is an upper limit to capacity and coverage achieved by DAS, depending on its noise figure.

(2) DAS systems are capacity limited on the reverse link due to the higher noise floor, attributed to the noise figure of the DAS.

7.2 Two Myths Busted

(1) Traditional network design is based on forward link capacity, relying on the fact that the reverse link is symmetrical. However DAS systems are reverse link limited and hence, DAS networks should be designed for reverse link capacity.

(2) Traditionally DAS design includes the use of a padding attenuator on the reverse link at the front end of the DAS in order to bring down the noise floor into the base station. It is clear from the analysis that this method has a negative impact on mobile transmit power and reduces the reverse link capacity and coverage.

7.3 Two Design suggestions

(1) Conventional base stations are designed to operate at a reduced noise floor level (on the order of -100 dBm). Without a padding attenuator, DAS systems cause the noise floor to rise and grow beyond the maximum received power limit. This forces the base station to operate non-linearly. Hence, base stations that are capable of operating in a higher noise floor, optimized for DAS systems, should be developed.

(2) As we saw, DAS antennas designed to operate in the entire cellular band are susceptible to out-of-band interference. Better automatic level control, whose response curves are configurable, should be developed so that they can be made to operate in a particular band only. This would help to eliminate the additional signal power which otherwise would be carried through the entire DAS chain up to the filter in front of the base station.

7.4 Two Open Issues

(1) BART spikes, as described in detail in the previous chapter, have not been observed in traditional CDMA cellular systems. The root cause for the reverse link channel imbalance, which results in the spikes, is an area that requires further attention and analysis.

(2) Unlike traditional single antenna systems, DAS systems are inherently capable of carrying multiple copies of the same signal transmitted by mobiles. Multiple signals can be utilized by the Rake receivers for their benefit if sufficient delay exists between the copies. Although several research papers have studied this in detail, analysis to measure and quantify the delay time on commercial DAS equipment has not been done. Introduction of a configurable delay element in DAS systems can result in more efficient utilization of multi-path environments.

Bibliography

[1] Victor L Granatstein. Physical Principles of Wireless Communications. Auerbach publications, 2008.

[2] Cdma2000 market trends and facts. Technical report, CDMA Development Group, August 2011.

[3] Femtocells and distributed antenna systems:complementary or competitive? Technical report, ABI Research, 2009.

[4] Evolution to lte and the surrounding challenges for in building coverage. Technical report, Zinwave Ltd, 2011.

[5] A.A.M. Saleh, A.J. Rustako, and R.S. Roman. Distributed antennas for indoor radio communications. IEEE Transactions on Communications, 35:12451251, December 1987.

[6] Distributed antenna systems - a national perspective. Technical report, The DAS Forum,New York State Wireless Association 2011 Trade Show and Conference Presentation, May 2011.

[7] L. Korowajczuk, B. Xavier, A. Filho, L. Ribeiro, C. Korowajczuk, and L. DaSilva. Designing cdma2000 Systems. John Wiley & Sons, Ltd., 2004.

[8] A. Salamasi and K. Gilhousen. On the system design aspects of code division multiple access (cdma) applied to digital cellular and personal communication networks. In Vehicular Technology Conference, 1991. Gateway to the Future Technology in Motion., 41st IEEE, pages 57–62, May 1991.

[9] J. Lee and L. Miller. CDMA Systems Engineering Handbook. Artech House Publications, 1998.

[10] Samuel C Yang. CDMA RF System Engineering. Artech House Publications, 1998.

[11] L. Greenstein, V. Erceg, Y. Yeh, and M. Clark. A new path-gain/delay-spread propagation model for digital cellular channels. IEEE Transactions on Vehicular Technology, 46(2):477 – 485, May 1997.

[12] A. Goldsmith. Wireless Communications. Cambridge University Press, 2005.

[13] V. Erceg, L. Greenstein, S. Tjandra, S. Parkoff, A. Gupta, B. Kulic, A. Julius, and R. Bianchi. An empirically based path loss model for wireless channels in suburban environments. IEEE Journal on Selected Areas in Communication, 17(7):1205 – 1211, July 1999.

[14] M. Hata. Empirical formula for propagation loss in land mobile radio services. IEEE Transactions on Vehicular Technology, 29(3):317–325, August 1980.

[15] Urban transmission loss models for mobile radio in the 900 and 1800 mhz bands. Technical report, European Cooperation in the Field of Scienti

c and Technical Research, EURO-COST 231, 1991. COST 231 TD (91) 73. Rev 2.

[16] J. Proakis. Digital Communications, 4th Ed. McGraw Hill, 2001.

[17] K. Kim and I. Koo. CDMA Systems Capacity Engineering. Artech House Publications, 2005.

[18] Telecommunications Industry Association, Washington DC. TIA/EIA/IS-95-A, Mobile Station-Base Station Compatibility Standard for Dual-Mode Wide band Spread Spectrum Cellular System, May 1995.

[19] Telecommunications Industry Association, Washington DC. TIA/EIA/IS-2000, cdma2000 Standard for Spread Spectrum Systems, August 2000.

[20] Telecommunications Industry Association, Washington DC. TIA/EIA/IS-856, cdma2000 High Rate Packet Data Air Interface Specification, November 2000.

[21] Telecommunications Industry Association, Washington DC. TIA-856-A, cdma2000 High Rate Packet Data Air Interface Specification, April 2004.

[22] Telecommunications Industry Association, Washington DC. TIA-856-B, cdma2000 High Rate Packet Data Air Interface Specification, October 2007.

[23] K. Gilhousen, I. Jacobs, R. Padovani, A. Viterbi, L. Weaver Jr., and C. Wheatley. On the capacity of a cellular cdma system. IEEE Transactions on Vehicular Technology, 40(2), May 1991.

[24] V. Paulrajan and J. Roberts. Capacity of a cdma cellular system with variable user data rates. In Global Telecommunication Conference (GLOBECOM), volume 3, pages 1458 – 1462, November 1996.

[25] A. Sampath, P. Sarath Kumar, and J. M. Holtzman. Power control and resource management for a multimedia cdma wireless system. In Sixth IEEE International Symposium on Personal, Indoor and Mobile Radio Communications, 1995. (PIMRC'95). 'Wireless: Merging onto the Information Superhighway', volume 1, pages 21–25, September 1995.

[26] J. Yang, Y. Choi, J. Ahn, and K. Kim. Capacity plane of cdma system for multimedia traffic. IEE Electronic Letters, pages 1432–1433, 1997.

[27] A. M. Viterbi and A. J. Viterbi. Erlang capacity of a power controlled cdma system. IEEE Journal on selected areas in Communications, 11(6), August 1993.

[28] A. Sampath, N. Mandayam, and J. M. Holtzman. Erlang capacity of a power controlled integrated voice and data cdma system. In IEEE Proceedings of Vehicular Technology Conference, pages 1557–1561, 1997.

[29] I. Koo, J. Yang, and K. Kim. Analysis of erlang capacity for ds-cdma systems supporting multi-class services with the limited number of channel elements. In IEEE Proceedings of Wireless Communications and Networking Conference, 2000 (WCNC2000), volume 1, pages 355 – 359, September 2000.

[30] I. Koo, J. Yang, K. Kim, and Y. Yang. An approximate analysis method of erlang capacity for cdma systems with multiple sectors and multiple frequency allocation bands. In IEEE Proceedings of Vehicular Technology Conference, 2001, volume 2, pages 926 – 930, May 2001.

[31] I. Koo, J. Yang, and K. Kim. Erlang capacity analysis of cdma systems supporting voice and delay-tolerant data services under the delay constraint. IEEE Transactions on Vehicular Technology, 56(4), July 2007.

[32] I. Koo, A. Ahmad, and K. Kim. Erlang capacity of cdma systems using optimized sectoring. International Journal of Wireless Information Networks, 10(2), April 2003.

[33] A. M. Viterbi, A. J. Viterbi, K. Gilhousen, and E. Zehavi. Soft hand-off extends cdma cell coverage and increases reverse link capacity. IEEE Journal on selected areas in Communications, 12(8), October 1994.

[34] D. Kim and F. Adachi. Theoretical analysis of reverse link capacity of an sir-based power-controlled cellular cdma system in a multi-path fading environment. IEEE Transactions on Vehicular Technology, 50(2), March 2001.

[35] T. Kawashima, V. Sharma, and A. Gersho. Capacity enhancement of cellular cdma by traffic based control of speech bit rate. IEEE Transactions on Vehicular Technology, 45(3):543 – 550, August 1996.

[36] J. Yu, Y. Yao, and J. Zhang. Reverse-link capacity of power-controlled cdma systems with beam forming. IEEE Transactions on Vehicular Technology, 53(5), September 2004.

[37] P. Chow, A. Karim, V. Fung, and C. Dietrich. Performance advantages of distributed antennas in indoor wireless communication systems. In IEEE Proceedings of Vehicular Technology Conference, 1994, volume 3, pages 1522 – 1526, June 1994.

[38] H. H. Xia, A. Herrera, S. Kim, and F. Rico. A cdma distributed antenna system for in building personal communication services. IEEE Journal on selected Areas in Communications, 14(4), May 1996.

[39] H. Yanikomeroglu and E. Sousa. Cdma distributed antenna system for indoor wireless communications. In IEEE Proceedings on Conference on Universal Personal Communications, 1993, volume 2, pages 990–994, October 1993.

[40] J. Yang. Analysis and simulation of a cdma pcs indoor system with distributed antennae. In Sixth IEEE International Symposium on Personal, Indoor and Mobile Radio Communications, 1995 (PIMRC'95), 'Wireless: Merging onto the Information Superhighway', volume 3, page 1123, September 1995.

[41] H. Zhuang, L. Dai, L. Xiao, and Y. Yao. Spectral efficiency of distributed antenna system with random antenna layout. IEEE Electronic Letters, 30(6):495–496, March 2003.

[42] Harold T. Friis. Noise figures of radio receivers. Proceedings of the IRE, 32(7):419–422, July 1944.

[43] K. Kerpez and S. Ariyavisitakul. A radio access system with distributed antennas. IEEE Transactions on Vehicular Technology, 45(2):265–275, May 1996.

[44] J. Wang and L.B. Milstein. Cdma overlay situations for microcellular mobile communications. IEEE Transactions on Communications, 43(234):603–614, April 1995.

[45] S. V. Hanly. Capacity and power control in spread spectrum macrodiversity radio networks. IEEE Transactions on Communications, 44(2):247–256, February 1996.

[46] H. Yanikomeroglu and E. Sousa. Power control and number of antenna elements in cdma distributed antenna systems. In IEEE Proceedings of Conference on Communications, 1998, volume 2, pages 1040–1045, June 1998.

[47] W. Roh and A. Paulraj. Outage performance of distributed antenna systems in a composite fading channel. In IEEE Proceedings of Vehicular Technology Conference, 2002, volume 3, pages 1520–1524, December 2002.

[48] M. V. Clark, T. M. Willis III, L. J. Greenstein, A. J. Rustako Jr., V. Erceg, and R. S. Roman. Distributed versus centralized antenna arrays in broadband wireless networks. In IEEE Proceedings of Vehicular Technology Conference, 2001, volume 1, pages 33–37, May 2001.

[49] G. Chen, C. Yu, and C. Huang. A simulation study of a distributed antenna-based cdma. In Seventh IEEE International Symposium on Personal, Indoor and Mobile Radio Communications, 1996 (PIMRC'96), volume 2, pages 517–521, October 1996.

[50] A. Obaid and H. Yanikomeroglu. Reverse-link power control in cdma distributed antenna systems. In IEEE Proceedings of Wireless Communications and Networking Conference, 2000 (WCNC2000), volume 2, pages 608–612, September 2000.

[51] L. Dai, S. Zhou, and Y. Yao. Capacity analysis in cdma distributed antenna systems. IEEE Transactions on Wireless Communications, 4(6):2613–2620, November 2005.

[52] E. Teletar. Capacity of multi-antenna gaussian channels. Technical report, AT&T Bell Labs, June 1995.

[53] W. Roh and A. Paulraj. Mimo channel capacity for the distributed antenna. In IEEE Proceedings of Vehicular Technology Conference, 2002, volume 2, pages 706–709, September 2002.

[54] H. Zhang and H. Dai. On the capacity of distributed mimo systems. In Conference on Information Sciences and Systems Proceedings, 2004 (CISS'04), March 2004.

[55] X. Chen, W. Fang, and L. Yang. Performance of multiple-input multiple-output wireless communications systems using distributed antennas. In IEEE Proceedings of Vehicular Technology Conference, 2005, volume 5, pages 3142 – 3146, June 2005.

[56] H. Dai. Distributed versus co-located mimo systems with correlated fading and shadowing. In IEEE International Conference on Acoustics, Speech and Signal Processing, 2006 (ICASSP'06), volume 4, May 2006.

[57] L. Xiao, L. Dai, H. Zhuang, S. Zhou, and Y. Yao. Information-theoretic capacity analysis in mimo distributed antenna systems. In IEEE Proceedings of Vehicular Technology Conference, 2003, volume 1, pages 779–782, April 2003.

[58] W. Choi, J.G. Andrews, and C. Yi. The capacity of multicellular distributed antenna networks. In International Conference on Wireless Networks Communication and Mobile Computing (WMCMC), 2005, volume 2, pages 1337–1342, June 2005.

[59] J. Park, E. Song, and W. Sung. Capacity analysis for distributed antenna systems using cooperative transmission schemes in fading channels. IEEE Transactions on Wireless Communications, 8(2):586 – 592, February 2009.

[60] X. You, D. Wang, B. Sheng, X. Gao, X. Zhao, and M. Chen. Cooperative distributed antenna systems for mobile communications (coordinated and distributed mimo). IEEE Wireless Communications Magazine, 17(3):35–43, June 2010.

[61] L. Yang and W. Fang. Performance of distributed-antenna ds-cdma systems over composite lognormal shadowing and nakagami-m-fading channels. IEEE Transactions on Vehicular Technology, 58(6):2872 – 2883, July 2009.

[62] H. Chen, J. Wang, and M. Chen. Performance analysis of the distributed antenna system with antenna selective transmission over generalized fading channels. In International Conference on Wireless Communications and Signal Processing (WCSP) Proceedings, 2009, pages 1–4, November 2009.

[63] H. Chen and M. Chen. Capacity of the distributed antenna systems over shadowed fading channels. In IEEE Vehicular Technology Conference 2009 Proceedings, pages 1–4, April 2009.

[64] L. Dai. A comparative study on uplink sum capacity with co-located and distributed antennas. IEEE Journal on selected areas in Communications, 29(6):1200 – 1213, June 2011.

[65] S. Firouzabadi and A. Goldsmith. Downlink performance and capacity of distributed antenna systems. CoRR, 2011.

[66] Cdma capacity and coverage. Technical report, ADC Telecommunications Inc, 2006.

[67] T. S. Rappaport. Wireless Communications: Principles and Practice. Prentice Hall, 2nd Edition, 2002.

[68] Agilent 8924c cdma mobile station test set. Technical report, Agilent Technologies Product Note, 2000.

[69] Telecommunications Industry Association, Washington DC. TIA-98-E, Recommended Minimum Performance Standards for Cdma2000 Spread Spectrum Mobile Stations, February 2003.

[70] B. Yuen. Base station closed-loop rf power control with lmv232 crest-factor invariant detector. Technical report, National Semiconductor Application Note 1433, January 2006.

[71] ZFL-1000LN+ Datasheet.

[72] Anritsu Spectrum Master MS2721B Technical Datasheet.